

Projected entangled pair states with continuous virtual symmetries

Henrik Dreyer, J. Ignacio Cirac, and Norbert Schuch

Max-Planck Institute of Quantum Optics, Hans-Kopfermann-Str. 1, 85748 Garching, Germany

(Received 8 June 2018; revised manuscript received 3 August 2018; published 12 September 2018)

We study projected entangled pair states (PEPS) with continuous virtual symmetries, i.e., symmetries in the virtual degrees of freedom, through an elementary class of models with $SU(2)$ symmetry. Discrete symmetries of that kind have previously allowed for a comprehensive explanation of topological order in the PEPS formalism. We construct local parent Hamiltonians whose ground space with open boundaries is exactly parametrized by the PEPS wave function, and show how the ground state can be made unique by a suitable choice of boundary conditions. We also find that these models exhibit a logarithmic correction to the entanglement entropy and an extensive ground space degeneracy on systems with periodic boundaries, which suggests that they do not describe conventional gapped topological phases, but either critical models or some other exotic phase.

DOI: [10.1103/PhysRevB.98.115120](https://doi.org/10.1103/PhysRevB.98.115120)**I. INTRODUCTION**

Tensor network states provide an entanglement-based description of wave functions of strongly correlated quantum systems. Besides being a powerful numerical tool, they also offer a systematic way of producing exact representations of quantum wave functions with a rich variety of behavior [1]. In one dimension, they have been used to completely classify phases resulting from both symmetry breaking and symmetry-protected topological order [2–4]. The full classification of phases in dimensions two and greater is currently still open, due in some part to the existence of phases with intrinsic topological order. Simple projected entangled pair state (PEPS) representations have been found, for example, for the toric code (and all other quantum double models) [5], string-net models [6,7], and fermionic states with chiral topological order [8–10]. The central role in all of these constructions is played by a *virtual symmetry* of the tensor, this is, a symmetry in the entanglement degrees of freedom. These symmetries, as well as symmetry twists, are locally undetectable yet show up in the global topological properties of the system: they allow to parametrize the ground space manifold, to study anyonic excitations and their statistics, and to determine the entanglement properties of the system.

So far, studies of PEPS with virtual symmetries have been restricted to models with discrete symmetry groups. Conversely, continuous symmetries are expected to give rise to qualitatively different behavior, as is apparent from other areas of many-body physics. Discrete symmetries can, for example, be spontaneously broken in less than three spatial dimensions at finite temperature, while continuous symmetries cannot [11]. In the context of virtual symmetries and topological order, this is particularly appealing. While the discrete symmetries hitherto studied have given a new perspective on known models in a tensor network framework, a new type of symmetry may correspond to unconventional phases beyond current knowledge.

In this paper, we initiate the study of PEPS with a continuous virtual symmetry. We focus on the symmetry group $SU(2)$ and its fundamental representation and study the most general PEPS with the simplest nontrivial virtual degrees of freedom,

in particular, its entanglement properties and the way in which it appears as a ground state of a local Hamiltonian. Specifically, we show how we can naturally define a parent Hamiltonian from the PEPS tensor on a 2×2 patch, and that the PEPS exactly parametrizes its ground space manifold on any region with open boundary conditions, an important property known as the *intersection property* in the PEPS literature [12]. Subsequently, we show that by a suitable choice of boundary terms, the parent Hamiltonian can be modified such as to exhibit a unique ground state in any finite volume. While this behavior is closely resemblant to that of PEPS with finite virtual symmetry group, we find that with periodic boundaries, the ground states cannot be parametrized purely in terms of symmetry twists, and the system keeps a ground space degeneracy which is *exponential* in the size of the boundary. A closer analysis reveals that there are at least two types of ground states: those which can be parameterized through symmetry twists and which span a space of linear dimension in the system size, and a distinct class of ground states which correspond to extremal “frozen” spin configurations, which are not coupled to other configurations by the Hamiltonian, and which contribute an exponential number of states. Finally, we also study the entanglement properties of PEPS wave functions with virtual $SU(2)$ symmetry and find that the system exhibits a logarithmic correction to the area law, as opposed to the constant correction for known gapped topological phases. Overall, this indicates a behavior that is clearly distinct of those of gapped topological phases with a finite number of anyons, which exhibit a finite ground space degeneracy and a constant correction to the entanglement entropy, and indicates either critical behavior of the system or some unconventional kind of order. We discuss possible interpretations of our findings in the conclusions.

II. THE WAVE FUNCTION

In this section, we define PEPS with $SU(2)$ symmetries, introduce the formalism used for their analysis, and analyze their entanglement properties.

A. Projected entangled pair states

Projected entangled pair states (PEPS) are created from an elementary 5-index tensor A_{uldr}^i , with the *physical index* $i = 1, \dots, d$ (with d the *physical dimension*) and the *virtual indices* $u, l, d, r = 1, \dots, D$ (with D the *bond dimension*). The tensor defines a *fiducial state*

$$|\psi_{1 \times 1}(A)\rangle = \begin{array}{c} | \\ \text{---} \boxed{A} \text{---} \\ | \end{array} = \sum_{iuldr} A_{uldr}^i |i\rangle |uldr\rangle, \quad (1)$$

where the box denotes both the tensor (with the legs the virtual indices) and the fiducial state. From the fiducial state, a family of states on the square lattice is generated by means of contraction,

$$|\psi_{2 \times 1}(A)\rangle = \begin{array}{c} | \\ \text{---} \boxed{A} \text{---} \\ | \end{array} \begin{array}{c} | \\ \text{---} \boxed{A} \text{---} \\ | \end{array} = \langle \phi^+ |_{r_1, l_2} |\psi_{1 \times 1}(A)\rangle \otimes |\psi_{1 \times 1}(A)\rangle, \quad (2)$$

where $|\phi^+\rangle = \sum_{i=1}^D |ii\rangle$, and so further for larger blocks.

Physical states are obtained by imposing boundary conditions $|X\rangle \in (\mathbb{C}^D)^{\otimes (2N_h + 2N_v)}$,

$$|\psi_{2 \times 1}(A, X)\rangle = \begin{array}{c} \partial u_1 \quad \partial u_2 \quad X \\ \begin{array}{|c|c|} \hline \begin{array}{c} u_1 \quad u_2 \\ \text{---} \boxed{A} \text{---} \boxed{A} \text{---} \\ d_1 \quad d_2 \end{array} \\ \hline \partial l_1 \quad \partial r_2 \\ \hline \partial d_1 \quad \partial d_2 \end{array} \\ \langle \phi^+ |_{\partial u_1, u_1} \langle \phi^+ |_{\partial u_2, u_2} \dots |\psi_{2 \times 1}(A)\rangle |X\rangle, \quad (3)$$

where $\partial u_1, \partial u_2, \dots$ are the indices of $|X\rangle$, u_1, u_2, \dots are the indices of $|\psi_{2 \times 1}(A)\rangle$ and the $\langle \phi^+ |$ contract them. A particular choice are periodic boundary conditions:

$$|X = \text{PBC}\rangle = |\phi^+ \rangle_{\partial u_1, \partial d_1} |\phi^+ \rangle_{\partial u_2, \partial d_2} \dots \quad (4)$$

B. A class of SU(2)-invariant PEPS

Given a unitary representation U_g of a group G , we say that a tensor is G -invariant if

$$\begin{array}{c} \downarrow \\ U_g \\ \downarrow \\ \begin{array}{c} \leftarrow U_g \quad \leftarrow \boxed{A} \quad \rightarrow U_g^\dagger \\ \leftarrow U_g^\dagger \quad \leftarrow \boxed{A} \quad \rightarrow U_g \end{array} \\ \downarrow \\ U_g^\dagger \\ \downarrow \end{array} = U_g \otimes U_g \otimes \overline{U_g} \otimes \overline{U_g} |\psi_{1 \times 1}(A)\rangle = |\psi_{1 \times 1}(A)\rangle \quad \forall g \in G. \quad (5)$$

Here, the arrows denote the direction in which the U_g and U_g^\dagger act on the tensor A . Previous studies of G -invariant PEPS

have focused on discrete groups G [5]. In the following, we generalize G invariance to the symmetry group $G = \text{SU}(2)$ and introduce a class of $\text{SU}(2)$ -invariant PEPS, which we subsequently study in detail.

We will focus on the case where $D = 2$, where $U_g \equiv g$ is the fundamental representation of $g \in \text{SU}(2)$. A basis for the two-dimensional subspace of $(\mathbb{C}^2)^{\otimes 4}$ that is invariant under $U_g \otimes U_g \otimes \overline{U_g} \otimes \overline{U_g}$ is given by $\{|w\rangle_{ul}|w\rangle_{dr}, |\phi^+\rangle_{ur}|\phi^+\rangle_{dl}\}$, where $|w\rangle = |01\rangle - |10\rangle$. Therefore, up to a constant factor, the most general fiducial state \tilde{A} is of the form

$$\begin{array}{c} | \\ \text{---} \boxed{\tilde{A}} \text{---} \\ | \end{array} = \lambda |0\rangle_p |w\rangle_{ul} |w\rangle_{dr} + |1\rangle_p |\phi^+\rangle_{ur} |\phi^+\rangle_{dl}, \quad (6)$$

where $\lambda \in \mathbb{C}$ and $|0\rangle$ and $|1\rangle$ are normalized and linearly independent, but not necessarily orthogonal.

A complication of the tensor \tilde{A} is that it involves different entangled states and is not rotationally invariant. We will now introduce another tensor A , which only requires one kind of entangled state, is rotationally invariant for $\lambda = 1$, yet generates the same family of states. Specifically, we will show that for any region, there exists an invertible operator B acting on the virtual indices at the boundary such that

$$|\psi_{N_h \times N_v}(A, X)\rangle = |\psi_{N_h \times N_v}(\tilde{A}, BX)\rangle. \quad (7)$$

In the special case of even N_h and N_v and periodic boundary conditions (PBC), $B|X = \text{PBC}\rangle = |X = \text{PBC}\rangle$. The price we pay is that A will no longer be explicitly $\text{SU}(2)$ -invariant. Yet, we will see that using A instead of \tilde{A} simplifies the majority of the derivations in this paper. Specifically, define

$$\begin{array}{c} | \\ \text{---} \boxed{A} \text{---} \\ | \end{array} = \lambda |0\rangle_p |\phi^+\rangle_{ul} |\phi^+\rangle_{dr} + |1\rangle_p |\phi^+\rangle_{ur} |\phi^+\rangle_{dl}. \quad (8)$$

The tensor A is clearly rotationally invariant for $\lambda = 1$.

To show Eq. (7), note that

$$\begin{array}{c} | \\ \text{---} \boxed{A} \text{---} \\ | \end{array} = \begin{array}{c} | \\ \text{---} \boxed{\tilde{A}} \text{---} \\ | \end{array} \begin{array}{c} Y \\ \circ \\ Y^\dagger \end{array} = \begin{array}{c} \circ \\ Y \\ \text{---} \boxed{\tilde{A}} \text{---} \\ \circ \\ Y^\dagger \end{array}, \quad (9)$$

where $Y = \begin{pmatrix} 0 & 1 \\ 1 & 0 \end{pmatrix}$ and all matrices act from left to right and from top to bottom. Inserting now the middle form of (9) into the even and the right-hand side into the odd sublattice of the

square lattice, we obtain

$$\begin{array}{c}
 \begin{array}{cc}
 \begin{array}{c} | \\ \square A \\ | \end{array} & \begin{array}{c} | \\ \square A \\ | \end{array} \\
 \square A & \square A \\
 \begin{array}{c} | \\ \square A \\ | \end{array} & \begin{array}{c} | \\ \square A \\ | \end{array}
 \end{array}
 =
 \begin{array}{c}
 \begin{array}{c} \circlearrowleft Y \\ | \\ \square \tilde{A} \\ | \end{array}
 \begin{array}{c} \circlearrowleft Y \\ \circlearrowleft Y \\ | \\ \square \tilde{A} \\ | \end{array}
 \begin{array}{c} | \\ \square \tilde{A} \\ | \end{array} \\
 \begin{array}{c} \circlearrowleft Y \\ | \\ \square \tilde{A} \\ | \end{array}
 \begin{array}{c} \circlearrowleft Y \\ \circlearrowleft Y \\ | \\ \square \tilde{A} \\ | \end{array}
 \begin{array}{c} \circlearrowleft Y \\ | \\ \square \tilde{A} \\ | \end{array}
 \end{array}
 =
 \begin{array}{c}
 \begin{array}{c} \circlearrowleft Y \\ | \\ \square \tilde{A} \\ | \end{array}
 \begin{array}{c} \circlearrowleft Y \\ | \\ \square \tilde{A} \\ | \end{array} \\
 \begin{array}{c} \circlearrowleft Y \\ | \\ \square \tilde{A} \\ | \end{array}
 \begin{array}{c} \circlearrowleft Y \\ | \\ \square \tilde{A} \\ | \end{array}
 \end{array}
, \quad (10)
 \end{array}$$

which proves (7) with

$$B = Y \otimes \mathbb{1} \otimes Y \otimes \mathbb{1} \cdots \otimes Y^T \otimes \mathbb{1} \otimes \cdots \quad (11)$$

The states generated by A are therefore equivalent to those generated by the $SU(2)$ -invariant tensor \tilde{A} up to invertible boundary terms which can be absorbed into the boundary conditions X . In the following, we will therefore work with the tensor A , and thus restrict to N_h , N_v even on PBC.

C. The loop picture

We will now introduce graphical notation that will provide a convenient way of expressing configurations of the PEPS through loop patterns. To this end, we introduce the rule

$$\begin{aligned}
 |0\rangle &\rightarrow |\square\rangle, \\
 |1\rangle &\rightarrow |\boxtimes\rangle.
 \end{aligned} \quad (12)$$

This prescription, e.g., leads to

$$\left. \begin{array}{cccc}
 1 & 0 & 1 & 0 \\
 0 & 1 & 1 & 1 \\
 1 & 0 & 0 & 0 \\
 1 & 1 & 0 & 1
 \end{array} \right\} \rightarrow \begin{array}{c} \text{Loop pattern} \end{array}. \quad (13)$$

To each such physical configuration corresponds a configuration of virtual states, obtained by contracting the tensors with the corresponding physical states on that patch with open boundaries (note that for $\langle 0|1\rangle \neq 0$, this requires projecting the physical state onto the *dual* basis vector). Since the virtual $|\phi^+\rangle$ form the same pattern as the \square and \boxtimes , and are connected by projecting onto $\langle \phi^+|$, which yet again yields $|\phi^+\rangle$, each open loop corresponds to a virtual state $|\phi^+\rangle$ at the corresponding virtual indices at the boundary, while each closed loop contributes a factor of 2 (due to our choice of normalization).

Let us now rigorously establish such a framework. In the following, we always consider an $N_h \times N_v$ patch. The degrees of freedom at the boundary are numbered from $1, \dots, 2N$, $N = N_h + N_v$, as shown in Fig. 1(a).

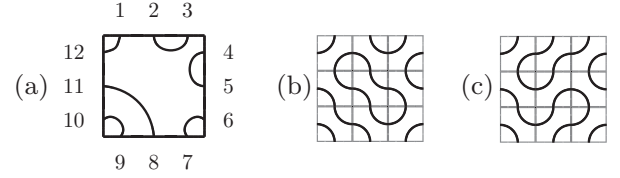


FIG. 1. Connectivity patterns and classes. (a) shows a connectivity pattern, here $\{(1, 12), (2, 3), (4, 5), (6, 7), (8, 11), (9, 10)\}$. (b) and (c) show two loop patterns which are compatible with the connectivity pattern in (a). All compatible patterns form the *connectivity class* corresponding to (a). For the loop pattern shown in (b), $n_L = 1$ and $b_L = 3$.

A *connectivity pattern* p on the boundary of the patch is a pairing of the numbers $1, \dots, 2N$, $N = N_h + N_v$, into noncrossing tuples $\{(a_1, b_1), \dots, (a_N, b_N)\}$, see Fig. 1(a).

A *loop pattern* L is a tiling of the patch with tiles \square and \boxtimes , such as in Figs. 1(b) and 1(c). To each loop pattern L , there is a corresponding *loop state* $|L\rangle$ of the physical system, namely the product state that is obtained by replacing \square with $|0\rangle$ and \boxtimes with $|1\rangle$. For a loop pattern L , we denote by n_L the number of closed loops in L and b_L is the number of \square -tiles in L . Each loop pattern L is *compatible* with a single connectivity pattern $p(L)$, namely, the one that is obtained by reading off the boundary pairs, which are connected by L . A *connectivity class* C_p for a given connectivity pattern is the set of all loop patterns which are compatible with p . We will denote the vector space spanned by all loop states $|L\rangle$ in the connectivity class C_p by $V(C_p)$.

A *boundary matching* is a state on the virtual degrees of freedom at the boundary corresponding to a connectivity pattern $p = \{(a_1, b_1), \dots, (a_N, b_N)\}$, that is,

$$|m(p)\rangle = |\phi^+\rangle_{a_1, b_1} \otimes \cdots \otimes |\phi^+\rangle_{a_N, b_N}. \quad (14)$$

This terminology permits us to write down the wave function of our PEPS in a concise way:

$$|\psi_{N_h \times N_v}(A)\rangle = \sum_{\substack{\text{connectivity} \\ \text{patterns} \\ p}} |m(p)\rangle \otimes \sum_{L \in C_p} |L\rangle 2^{n_L} \lambda^{b_L}. \quad (15)$$

The proof is immediate from the definition of the tensors, and the fact that each closed loop contributes a factor of 2, as discussed above.

The set of all boundary matchings $|m(p)\rangle$ is linearly independent and forms a basis of the space of all staggered spin 0 states (i.e., spin 0 up to a action of Y on every second site). This can be seen as follows: different $|m(p)\rangle$ correspond to different noncrossing partitions of the boundary points into pairs, which form maximally entangled states. Application of Y on every other boundary site turns such a matching of $|\phi^+\rangle$ into a matching of singlets, i.e.,

$$\begin{aligned}
 Y \otimes \mathbb{1} \otimes \cdots \otimes Y \otimes \mathbb{1} |\phi^+\rangle_{a_1, b_1} \otimes \cdots \otimes |\phi^+\rangle_{a_N, b_N} \\
 = |w\rangle_{a_1, b_1} \otimes \cdots \otimes |w\rangle_{a_N, b_N}.
 \end{aligned} \quad (16)$$

The set of noncrossing singlet matchings is a minimal basis for the spin 0 space, in particular, the matchings are mutually

linearly independent as shown in Refs. [13–15]. Indeed, there this is proven as follows. First, all singlet matchings, noncrossing or otherwise, form an overcomplete basis of the spin 0 space. However, each crossing matching can be “uncrossed” using the relation

$$\begin{array}{c} \diagup \diagdown \\ \diagdown \diagup \end{array} = \frac{1}{2} \begin{array}{c} \text{---} \\ \text{---} \end{array} + \frac{1}{2} \begin{array}{c} | \\ | \end{array}, \quad (17)$$

where the points are spin-1/2 particles and the lines indicate singlet pairings with a suitably chosen orientation. Using this relation iteratively, one can express every spin 0 state as a superposition of crossing-free singlet pairings. Since there are $\frac{1}{N+1} \binom{2N}{N}$ noncrossing matchings which coincides with the dimension of the spin 0 subspace of $2N$ qubits, these form a minimal basis. Since $Y \otimes \mathbb{1} \otimes \dots \otimes Y \otimes \mathbb{1}$ is an invertible operator, the $|m(p)\rangle$ form a minimal basis of the staggered spin 0 space.

This implies two things. First, we can restrict any boundary condition X to the staggered spin 0 space. Second, there exists a dual basis $\{|m^*(p)\rangle\}_p$ of that space such that $\langle m^*(p)|m(q)\rangle = \delta_{pq}$.

Using the dual basis, we can construct states that are superpositions of all loop patterns in the same connectivity class,

$$|\psi_{N_h \times N_v}(A, X = |m^*(p)\rangle)\rangle = \sum_{L \in C_p} |L\rangle 2^{n_L} \lambda^{b_L}. \quad (18)$$

For instance, for $p = \begin{array}{c} \text{---} \\ \text{---} \end{array}$ and $\lambda = 1$,

$$|\psi_{3 \times 3}(A, X = |m^*(p)\rangle)\rangle = 2 \begin{array}{c} \text{---} \\ \text{---} \end{array} + \begin{array}{c} \text{---} \\ \text{---} \end{array} + \dots \quad (19)$$

Moreover, since $\{|m^*(p)\rangle_p\}$ forms a basis of the space of staggered singlets (and thus of all relevant boundary conditions), we can express the PEPS obtained from any boundary condition X as

$$\begin{aligned} |\psi_{N_h \times N_v}(A, X)\rangle &= \sum_p \langle X|m(p)\rangle \sum_{L \in C_p} |L\rangle 2^{n_L} \lambda^{b_L} \\ &= \sum_p \langle X|m(p)\rangle |\psi_{N_h \times N_v}(A, |m^*(p)\rangle)\rangle. \end{aligned} \quad (20)$$

D. Configuration counting

In the following, we will determine the dimension of the space

$$\mathcal{S}_{N_h \times N_v} := \text{span}\{|\psi_{N_h \times N_v}(A, X)\rangle | X \in \mathbb{C}^{2N_h + 2N_v}\} \quad (21)$$

of all physical configurations accessible with our tensor network. This on the one hand will be relevant when computing the entanglement entropy in Sec. II E, and on the other hand, when determining the ground space degeneracy with open boundaries in Sec. III. As we have just seen in Eq. (20), $\mathcal{S}_{N_h \times N_v}$ is spanned exactly by the states given in (18).

These states are linearly independent—unless they are zero—due to the linear independence of different $|L\rangle$, which follows from the linear independence of $|0\rangle$ and $|1\rangle$. In order for Eq. (18) to be nonzero for a given connectivity pattern p ,

it must hold that C_p is nonempty. We will call connectivity patterns p for which C_p is empty *forbidden*, otherwise we call p *allowed*.

An example of a forbidden connectivity pattern on a 2×2 patch is

$$\begin{array}{c} | \\ | \end{array}. \quad (22)$$

The intuitive reason for this connectivity class to be empty is the fact that it requests too large amounts of entanglement between the upper and lower boundary of the system, more than can be mediated by the bulk: the connectivity pattern requires four maximally entangled states between top and bottom half, while the PEPS only has two bonds along that cut. If we tried to find a loop pattern that matches the connectivity pattern, we would see that the first two north-south connections fill up all available space:

$$\begin{array}{c} | \\ | \end{array}. \quad (23)$$

In order to compute the dimension of $\mathcal{S}_{N_h \times N_v}$, we therefore need to determine the number of allowed connectivity patterns for that given system size, which we denote by $\mathcal{N}(N_h, N_v)$. The explicit form of this number is constructed in Appendix B, and given in Eqs. (B5) and (B6). For the main statements of this paper, the asymptotic behavior will be sufficient. If we take N_h and N_v to the thermodynamic limit in a fixed aspect ratio $N_v/N_h =: \alpha - 1$, then [as proven in Appendix B, Eq. (B40)] the asymptotic behavior is essentially that of the Catalan numbers. Specifically, denoting the size of the boundary by $N = N_h + N_v$, we find that \mathcal{N} scales asymptotically as

$$\mathcal{N}(\alpha, N) = \frac{4^N}{N^{3/2}} \left[k(\alpha) + \mathcal{O}\left(\frac{1}{N}\right) \right] \quad (24)$$

with $k(\alpha)$ a function of the aspect ratio which is independent of N .

E. Entanglement entropy

We are now ready to determine the scaling behavior of the entanglement in our model. To this end, consider a partition of the $N_h \times N_v$ torus into a (small) rectangle Q of size $L_h \times L_v$, and the (large) rest R . Our goal is to determine the zero Renyi entropy $S_0(\rho_Q)$ of the reduced state on Q , that is, the logarithm of the Schmidt rank of $|\psi_{N_h \times N_v}(A, PBC)\rangle$ in said partition. To this end, note that by construction

$$|\psi_{N_h \times N_v}(A, PBC)\rangle = (\Psi_Q \otimes \Psi_R) |\phi^+\rangle^{|\partial Q|}, \quad (25)$$

where Ψ_Q is the linear map $|\psi_{L_h \times L_v}(A, \bullet)\rangle$ from the boundary to the bulk in Q and correspondingly for Ψ_R , and the $|\phi^+\rangle^{|\partial Q|}$ are placed along the boundary between Q and R , which has length $|\partial Q| = 2L_h + 2L_v =: L$.

As we have seen in the preceding section, the map Ψ_Q provides a bijection between the space $\mathcal{V}_{\text{allowed}}$ spanned by all $|m^*(p)\rangle$ with p an allowed matching, and its image $\mathcal{S}_{L_h \times L_v}$. Ψ_R , on the other hand, provides a bijection between the full staggered spin 0 space \mathcal{V}_0 and its image in R , as long as Q is sufficiently small [specifically, if $\min\{N_h, N_v\} > \frac{3}{2}(L_h + L_v)$], as in that case there are no forbidden matchings. Intuitively, this

follows from the fact that forbidden matchings arise due to space constraints at the corners, and the region Q is concave; we provide a proof in Appendix C.

Thus, up to these bijections, $|\psi_{N_h \times N_v}(A, \text{PBC})\rangle$ equals $(\Pi_{\mathcal{V}_{\text{allowed}}} \otimes \Pi_{\mathcal{V}_0})|\phi^+\rangle^{|\partial Q|}$, which has Schmidt rank equal to $\dim \mathcal{V}_{\text{allowed}} = \mathcal{N}(L_h, L_v)$. Using (24), we obtain that for a fixed aspect ratio of Q , $S_0(\rho_Q)$ scales as

$$S_0(\rho_Q) = L \ln 2 - \frac{3}{2} \ln(L/2) + \ln k + \mathcal{O}\left(\frac{1}{L}\right) \quad (26)$$

with a nonuniversal constant $\ln k$ that depends on the aspect ratio of Q .

As expected, the first term corresponds to the area law $|\partial Q| \ln D$, D being the bond dimension of the PEPS. Nevertheless, the subleading term is logarithmic rather than a constant as in topologically ordered models. Such corrections have been investigated in Ref. [16]. There, entropies for conformal two-dimensional quantum critical points, like the quantum dimer [17,18] and the quantum eight-vertex model [19] have been studied. The authors find a universal logarithmic correction to the area law, which depends on the associated conformal field theory and the geometrical details of the partition. In particular, the same theory can have a pure area law for region A being a disk, while for A rectangular, logarithmic corrections appear. Similarly, in our case, the notion of allowed and forbidden connectivity patterns—which is fundamental to our calculation—depends on the shape of the partition. Curiously, the models studied in [16] were found to lie at the boundary of topologically ordered phases [20].

III. PARENT HAMILTONIANS

In the following, we will study how our $SU(2)$ -invariant wave function can appear as a ground state. To this end, we will construct a local parent Hamiltonian and subsequently characterize its ground space, both for open boundary conditions (OBC) and on the torus. In particular, we will show that the parent Hamiltonian possesses a property known as *intersection property* [2,12], and that we can obtain a unique ground state with OBC by gapping out the boundary. In the following, we will focus on the case $\lambda = 1$.

A. Construction of the Hamiltonian and intersection property

Parent Hamiltonians for PEPS are constructed by taking a plaquette of spins and finding a positive operator that annihilates any state that looks like the PEPS on that patch, while penalizing orthogonal states. In our case, the Hamiltonian acts on a 2×2 plaquette. To this end, define

$$\mathcal{S}_{2 \times 2} := \text{span} \left\{ \left[\begin{array}{c} \text{Diagram of a } 2 \times 2 \text{ plaquette with four } A \text{ sites and } X \text{ boundary} \\ \left| X \in (\mathbb{C}^2)^{\otimes 8} \right. \end{array} \right. \right\} \quad (27)$$

and set

$$h = \mathbb{1} - \Pi_{\mathcal{S}_{2 \times 2}} \quad (28)$$

to be the projector onto the orthogonal complement of $\mathcal{S}_{2 \times 2}$. For any patch, we can then define

$$H = \sum_{x,y} h_{(x,y)}, \quad (29)$$

where (x, y) is the top left spin of $h_{(x,y)}$, and the sum runs over all x and y on the patch, according to the chosen boundary conditions. By construction, $H \geq 0$ and $h_{(x,y)}|\psi_{N_x \times N_y}(A, X)\rangle = 0$ for all X , and thus, any $|\psi_{N_x \times N_y}(A, X)\rangle$ is a ground state of H . The remaining question is thus to understand whether these states fully span the ground space of H . For OBC, this is known as the *intersection property* (that is, the intersection of the ground spaces of the $h_{(x,y)}$ is given by the PEPS with arbitrary boundary on the larger patch).

In order to understand the structure of an arbitrary ground state of H , let us consider the action of h in terms of the loop picture. It is convenient to introduce the following notation for loop states on 2×2 plaquettes:

$$\begin{aligned} & \left| \begin{array}{c} \text{Diagram of a } 2 \times 2 \text{ plaquette with a central bubble} \\ \left| B \right. \end{array} \right\rangle = |B\rangle, \\ & \left| \begin{array}{c} \text{Diagram of a } 2 \times 2 \text{ plaquette with a tadpole} \\ \left| E_1 \right. \end{array} \right\rangle = |E_1\rangle, \quad \left| \begin{array}{c} \text{Diagram of a } 2 \times 2 \text{ plaquette with a tadpole} \\ \left| E_2 \right. \end{array} \right\rangle = |E_2\rangle, \\ & \left| \begin{array}{c} \text{Diagram of a } 2 \times 2 \text{ plaquette with a tadpole} \\ \left| E_3 \right. \end{array} \right\rangle = |E_3\rangle, \quad \left| \begin{array}{c} \text{Diagram of a } 2 \times 2 \text{ plaquette with a tadpole} \\ \left| E_4 \right. \end{array} \right\rangle = |E_4\rangle, \\ & \left| \begin{array}{c} \text{Diagram of a } 2 \times 2 \text{ plaquette with a tadpole} \\ \left| O_1 \right. \end{array} \right\rangle = |O_1\rangle, \quad \left| \begin{array}{c} \text{Diagram of a } 2 \times 2 \text{ plaquette with a tadpole} \\ \left| O_2 \right. \end{array} \right\rangle = |O_2\rangle, \quad \left| \begin{array}{c} \text{Diagram of a } 2 \times 2 \text{ plaquette with a tadpole} \\ \left| O_3 \right. \end{array} \right\rangle = |O_3\rangle, \\ & \left| \begin{array}{c} \text{Diagram of a } 2 \times 2 \text{ plaquette with a tadpole} \\ \left| O_4 \right. \end{array} \right\rangle = |O_4\rangle, \quad \left| \begin{array}{c} \text{Diagram of a } 2 \times 2 \text{ plaquette with a tadpole} \\ \left| O_5 \right. \end{array} \right\rangle = |O_5\rangle, \quad \left| \begin{array}{c} \text{Diagram of a } 2 \times 2 \text{ plaquette with a tadpole} \\ \left| O_6 \right. \end{array} \right\rangle = |O_6\rangle, \\ & \left| \begin{array}{c} \text{Diagram of a } 2 \times 2 \text{ plaquette with a tadpole} \\ \left| O_7 \right. \end{array} \right\rangle = |O_7\rangle, \quad \left| \begin{array}{c} \text{Diagram of a } 2 \times 2 \text{ plaquette with a tadpole} \\ \left| O_8 \right. \end{array} \right\rangle = |O_8\rangle, \quad \left| \begin{array}{c} \text{Diagram of a } 2 \times 2 \text{ plaquette with a tadpole} \\ \left| O_9 \right. \end{array} \right\rangle = |O_9\rangle, \\ & \left| \begin{array}{c} \text{Diagram of a } 2 \times 2 \text{ plaquette with a tadpole} \\ \left| O_{10} \right. \end{array} \right\rangle = |O_{10}\rangle, \quad \left| \begin{array}{c} \text{Diagram of a } 2 \times 2 \text{ plaquette with a tadpole} \\ \left| O_{11} \right. \end{array} \right\rangle = |O_{11}\rangle. \end{aligned} \quad (30)$$

We will refer to $|B\rangle$ as *bubbles*, $|E_i\rangle$ as *tadpoles*, and $|O_i\rangle$ as *bubble-free states*. Furthermore, define

$$|\phi\rangle = \frac{1}{2\sqrt{2}} \left[2|B\rangle + \sum_{i=1}^4 |E_i\rangle \right]. \quad (31)$$

Then, each local term has 12 possible ground states:

$$|O_i\rangle, \quad i = 1, \dots, 11 \quad \text{and} \quad |\phi\rangle. \quad (32)$$

Taking a general state $|g\rangle = \sum_i o_i |O_i\rangle + \sum_i e_i |E_i\rangle + b|B\rangle$, a direct calculation reveals that $h|g\rangle = 0$ if and only if $e_i = e_j \forall i, j$ and $e_i = b/2 \forall i$. That is, in order to be a ground state

of h , the states $|B\rangle$ and $|E_i\rangle$ must appear with the relative amplitudes $2 : 1 : 1 : 1 : 1$, as in $|\phi\rangle$ —and this is the *only* condition in order to be a ground state.

We can thus interpret the Hamiltonian as defining a random walk on the space of loop configurations,

$$2 \begin{array}{c} \begin{array}{|c|c|c|c|} \hline \circ & \circ & \circ & \circ \\ \hline \end{array} \\ \Leftrightarrow \\ \begin{array}{|c|c|c|c|} \hline \circ & \circ & \circ & \circ \\ \hline \end{array} \\ \Leftrightarrow \\ \begin{array}{|c|c|c|c|} \hline \circ & \circ & \circ & \circ \\ \hline \end{array} \\ \Leftrightarrow \\ \begin{array}{|c|c|c|c|} \hline \circ & \circ & \circ & \circ \\ \hline \end{array} \\ \Leftrightarrow \\ \begin{array}{|c|c|c|c|} \hline \circ & \circ & \circ & \circ \\ \hline \end{array} \end{array}, \quad (33)$$

i.e., any two states coupled by the transition (33) must appear in any ground state in superposition with the given relative amplitude. Differently speaking, for any orbit of the random walk (33) acting on all sites, there is at most one ground state per orbit. In the following, we will call such a move between loop configurations a *surgery move* and use the notation $L' = \sigma(L)$ to describe the fact that loop patterns L' and L are related by such a move. We will denote *sequences* of surgery moves by capital letters, e.g., $\Sigma = \sigma_1 \dots \sigma_M$.

We will now use this interpretation to prove that for H on an OBC rectangle, there is exactly one ground state per connectivity pattern, that is, the ground space is given by

$$\mathcal{S}_{N_h \times N_v} := \text{span} \left\{ |\psi_{N_h \times N_v}(A, X)\rangle \mid X \in \mathbb{C}^{(2N_h + 2N_v)} \right\},$$

this is precisely the intersection property. In particular, it entails that the degeneracy of the parent Hamiltonian is given by $\mathcal{N}(N_h, N_v)$.

To start with, note that each surgery move leaves the connectivity pattern invariant, i.e., $\langle K | h | L \rangle = 0$ if $K \in C_p \neq C_q \ni L$. The Hamiltonian is therefore block diagonal in the loop basis,

$$H = \bigoplus_p H_p, \quad (34)$$

where the H_p are supported on $V(C_p)$. Now pick the basis $|\psi_p\rangle := \{|\psi_{N_h \times N_v}(A, m^*(p))\rangle\}_p$ of $\mathcal{S}_{N_h \times N_v}$, cf. Eq. (18). Each of these states is by construction a ground state of H , and lives in the corresponding block $V(C_p)$ of the Hamiltonian. It thus remains to show that the random walk defined by H couples any two configurations $L, L' \in C_p$. As argued above, this uniquely fixes the ratios of the coefficients $\sum_{L \in C_p} c_L |L\rangle$ for any given p , which thus must be equal to those of $|\psi_p\rangle$. [Note that the fact that $|\psi_p\rangle$ is a ground state implies that the ratio must be independent of the chosen path $\Sigma(L) = L'$ of surgery moves.] Indeed, as we show in Appendices A and D, for any given connectivity pattern p , we can define a canonical pattern L_0 such that any $L \in C_p$ can be connected to L_0 through a sequence Σ_0 of surgery moves, $L_0 = \Sigma_0(L)$, and thus, any two $L, L' \in C_p$ are connected through a sequence Σ that goes through L_0 ,

$$L = \Sigma_0^{-1}(\Sigma'_0(L')), \quad (35)$$

where $L_0 = \Sigma'_0(L')$. Differently speaking, the random walk (33) is ergodic in the space of loop states with a fixed connectivity pattern.

This implies that (up to normalisation), on a OBC patch of size $N_h \times N_v$,

$$|\psi_p\rangle = \sum_{L \in C_p} 2^{n_L} |L\rangle \quad (36)$$

is the unique ground state of H in sector p , i.e., H has one ground state per connectivity pattern C_p , and the space of all ground states is given by $\mathcal{S}_{N_h \times N_v}$.

B. Open boundary conditions and unique ground state

We have just seen that the parent Hamiltonian possesses the intersection property—the ground space manifold on any rectangular patch is precisely given by those configurations that can be obtained by choosing arbitrary boundary conditions. In the following, we will show that, for N_h, N_v even, it is possible to gap out the boundary, that is, to add boundary terms to the parent Hamiltonian which yield a unique ground state.

To this end, we target

$$|\psi\rangle = \begin{array}{c} \begin{array}{|c|c|} \hline A & A \\ \hline \end{array} \dots \begin{array}{|c|c|} \hline A & A \\ \hline \end{array} \\ \vdots \\ \begin{array}{|c|c|} \hline A & A \\ \hline \end{array} \dots \begin{array}{|c|c|} \hline A & A \\ \hline \end{array} \end{array} \quad (37)$$

as the unique ground state, and proceed by constructing its parent Hamiltonian. In the bulk, the parent Hamiltonian will be the same as before. On the boundary, however, extra terms appear. Specifically, we consider a 2×1 tile

$$\begin{array}{|c|c|} \hline \circ & \circ \\ \hline \end{array} \quad (38)$$

at either boundary, and define

$$\mathcal{R}_{(2n-1,1),(2n,1)} := \text{span} \left\{ \begin{array}{|c|c|} \hline \begin{array}{|c|c|} \hline A & A \\ \hline \end{array} \\ \hline \end{array} \mid X \in (\mathbb{C}^2)^{\otimes 4} \right\} \quad (39)$$

(and rotated versions thereof) and the corresponding parent Hamiltonian

$$h'_{(x_1,y_1),(x_2,y_2)} = \mathbb{1} - \Pi_{\mathcal{R}_{(x_1,y_1),(x_2,y_2)}}. \quad (40)$$

It is easy to check that h' , together with the original parent Hamiltonian on the corresponding 2×2 patch, has exactly the same ground space as the “true” parent Hamiltonian derived from that patch of $|\psi\rangle$ including the boundary condition (and containment, which suffices for $|\psi\rangle$ to be a ground state, holds trivially). On the other hand, the parent Hamiltonians on the shifted patches remain unchanged. Thus

$$\begin{aligned} H' := H &+ \sum_{n=1}^{N_h/2} [h'_{(2n-1,1),(2n,1)} + h'_{(2n-1,N_v),(2n,N_v)}] \\ &+ \sum_{n=1}^{N_v/2} [h'_{(1,2n-1),(1,2n)} + h'_{(N_h,2n-1),(N_h,2n)}] \end{aligned} \quad (41)$$

is a parent Hamiltonian of $|\psi\rangle$ and has $|\psi\rangle$ as a ground state.

Let us now show that this ground state is unique. To this end, note that the ground space of h' on a 2×1 patch is spanned by the states

$$\begin{aligned} |\theta_1\rangle &= \begin{array}{|c|c|} \hline \circ & \circ \\ \hline \end{array} + \begin{array}{|c|c|} \hline \circ & \circ \\ \hline \end{array} + 2 \begin{array}{|c|c|} \hline \circ & \circ \\ \hline \end{array}, \\ |\theta_2\rangle &= \begin{array}{|c|c|} \hline \circ & \circ \\ \hline \end{array}. \end{aligned} \quad (42)$$

Thus h' imposes the additional constraint that in any ground state the states in $|\theta_1\rangle$ must appear as superpositions with the corresponding weights. Arguing as before, this fixes the relative amplitudes of any two loop patterns coupled by the additional surgery move

$$\begin{array}{|c|c|} \hline \diagup \diagdown \\ \hline \end{array} \Leftrightarrow \begin{array}{|c|c|} \hline \diagdown \diagup \\ \hline \end{array} \Leftrightarrow 2 \begin{array}{|c|c|} \hline \diagup \diagup \\ \hline \end{array} \quad (43)$$

on the corresponding 2×1 patches, and rotated versions thereof.

As we show in Appendix F, any loop pattern can be transformed to a loop pattern in the ‘‘minimal’’ connectivity class

$$p_{\min} = \begin{array}{|c|} \hline \square \\ \hline \end{array} \quad (44)$$

by using the original (bulk) surgery moves, together with the additional surgery move (43) obtained from h' (which allows to change the connectivity class). On the other hand, we have seen in Sec. III A that any two loop patterns in a given connectivity class—specifically, the minimal one above—are connected through bulk surgery moves. Thus, it follows that any two loop patterns can be connected by combining bulk and boundary surgery moves, and thus, the relative amplitudes of all loop patterns are fixed and therefore equal to those found in $|\psi\rangle$, Eq. (37). We thus infer that $|\psi\rangle$ is the unique ground state of H' .

C. Periodic boundary conditions

Let us now study the ground space structure of the parent Hamiltonian (29) on a system with periodic boundary conditions (PBC); recall from Sec. II that this requires N_h and N_v to be even. To this end, we will resort to the description of the PEPS in terms of the tensor \tilde{A} , Eq. (6), rather than A (see Sec. II B). Note that due to the gauge relation (7) between them, both A and \tilde{A} have the same parent Hamiltonian as defined in (28).

Let us first consider an approach that allowed to fully characterize the ground space for G -injective PEPS with finite symmetry group G [5]. (In the following, all arrows point from left to right and top to bottom by convention.) First, note that the fundamental symmetry (5) is stable under concatenation, e.g.,

$$\begin{array}{|c|} \hline U_g \\ \hline \tilde{A} \\ \hline U_g^\dagger \\ \hline \end{array} \begin{array}{|c|} \hline U_g \\ \hline \tilde{A} \\ \hline U_g^\dagger \\ \hline \end{array} = \begin{array}{|c|} \hline U_g \\ \hline \tilde{A} \\ \hline U_g^\dagger \\ \hline \end{array} \begin{array}{|c|} \hline U_g \\ \hline U_g^\dagger \\ \hline \end{array} \begin{array}{|c|} \hline U_g \\ \hline \tilde{A} \\ \hline U_g^\dagger \\ \hline \end{array} \begin{array}{|c|} \hline U_g \\ \hline U_g^\dagger \\ \hline \end{array} \\ \\ = \begin{array}{|c|} \hline \tilde{A} \\ \hline \end{array} \begin{array}{|c|} \hline \tilde{A} \\ \hline \end{array} , \quad (45)$$

i.e., any closed loop of symmetry operators leaves a simply connected patch invariant. This is particularly interesting when

we consider closed boundary conditions:

$$\begin{array}{|c|} \hline U_g^\dagger \\ \hline \tilde{A} \\ \hline U_g^\dagger \\ \hline \end{array} = \begin{array}{|c|} \hline U_g \\ \hline U_g \\ \hline \tilde{A} \\ \hline U_g \\ \hline U_g \\ \hline U_g^\dagger \\ \hline U_g^\dagger \\ \hline \end{array} = \begin{array}{|c|} \hline U_g^\dagger \\ \hline \tilde{A} \\ \hline U_g^\dagger \\ \hline \end{array} . \quad (46)$$

Virtual string operators of the form $U_g^{\otimes N_v}$, which wrap vertically around the torus, can therefore be freely moved around the torus, and correspondingly horizontal loops $V_h^{\otimes N_h}$, i.e., the state

$$|\psi_{N_h \times N_v}\{U_g, V_h\}\rangle = \dots \begin{array}{|c|} \hline U_g \\ \hline U_g \\ \hline U_g \\ \hline U_g \\ \hline V_h \\ \hline V_h \\ \hline V_h \\ \hline V_h \\ \hline \end{array} \dots \quad (47)$$

on the torus is independent of the position of the strings, as long as $[U_g, V_h] = 0$ (otherwise, the strings might not be movable where they intersect).

It is now clear that any such state $|\psi_{N_h \times N_v}\{U_g, V_h\}\rangle$ is a ground state of the parent Hamiltonian $H = \sum h_{(x,y)}$, since for any local term $h_{(x,y)}$, the strings can be moved such that they are outside the region where $h_{(x,y)}$ acts. In the case of G -injective PEPS with finite symmetry group, it could be shown that these states precisely parametrize the full ground space of H [5]. For Abelian groups, all (g, h) yield linearly independent ground states $|\psi_{N_h \times N_v}\{U_g, V_h\}\rangle$, while for non-Abelian groups, linear dependencies arise as certain (g, h) yield identical states.

Let us now consider the case of $G = SU(2)$. Clearly,

$$S' = \text{span}\{|\psi_{N_h \times N_v}\{U, V\}\rangle \mid U, V \in SU(2), [U, V] = 0\} \quad (48)$$

is inside the ground space of H . What is the dimension of S' ? Without loss of generality, we can restrict to $U = \text{diag}(e^{i\phi}, e^{-i\phi})$ —otherwise, we conjugate each \tilde{A} with the unitary which diagonalises U , leaving the state invariant. Then (up to basis permutations),

$$U^{\otimes N_v} = e^{iN_v\phi} \mathbb{1}_{\binom{N_v}{0}} \oplus e^{i(N_v-2)\phi} \mathbb{1}_{\binom{N_v}{1}} \oplus \dots \oplus e^{-iN_v\phi} \mathbb{1}_{\binom{N_v}{N_v}}, \quad (49)$$

for arbitrary values of ϕ , and thus, the closure $U_g^{\otimes N_v}$ on its own parametrizes a $(N_v + 1)$ -dimensional subspace (e.g. by choosing Fourier angles $\phi_k = 2\pi k / (2N_v + 1)$, $k = -N_v/2, \dots, N_v/2$). In order to satisfy $[U, V] = 0$, we must have $V = \text{diag}(e^{i\theta}, e^{-i\theta})$, and thus, S' is at most $(N_h + 1)(N_v + 1)$ -dimensional. However, it is easy to see that there is at least one more redundancy: by conjugating each \tilde{A} with the Pauli X operator, we map $\phi \rightarrow -\phi, \theta \rightarrow -\theta$. This reduces the

number of possibilities by a factor of 2, except at $\phi = \theta = 0$. As we show in Appendix G, the remaining states are indeed linearly independent, and thus,

$$\dim \mathcal{S}' = \frac{(N_h + 1)(N_v + 1) + 1}{2}.$$

One might think that this parameterizes the full ground space of H , just as for G -injective PEPS with finite G . However, this is not the case. To see this, consider an arbitrary bit-string $b \in \{0, 1\}^{N_h}$. Then, we define the product state $|v(b)\rangle$ by stacking N_v copies of b on top of each other and then identifying $0 \rightarrow |0\rangle$ and $1 \rightarrow |1\rangle$, for example,

$$|v(0101)\rangle = \begin{array}{|c|c|c|c|} \hline \text{---} & \text{---} & \text{---} & \text{---} \\ \hline \text{---} & \text{---} & \text{---} & \text{---} \\ \hline \text{---} & \text{---} & \text{---} & \text{---} \\ \hline \text{---} & \text{---} & \text{---} & \text{---} \\ \hline \end{array}. \quad (50)$$

Horizontally stacked states $|h(b)\rangle$ are defined accordingly. Clearly, there are $2^{N_h} + 2^{N_v} - 2$ of these states (since only the all-0 and all-1 states are doubly counted). Finally, all of them are ground states, since, by definition, no plaquette locally looks like any of $|B\rangle = \begin{smallmatrix} 0 \\ 1 \end{smallmatrix}$, $|E_1\rangle = \begin{smallmatrix} 0 & 0 \\ 1 & 0 \end{smallmatrix}$, $|E_2\rangle = \begin{smallmatrix} 0 & 1 \\ 0 & 0 \end{smallmatrix}$,

$|E_3\rangle = \begin{smallmatrix} 1 \\ 1 \end{smallmatrix}$ or $|E_4\rangle = \begin{smallmatrix} 0 & 1 \\ 1 & 1 \end{smallmatrix}$, even across the boundary. Note that in all of these configurations, the winding of the loops around the torus is maximal in at least one direction (horizontally or vertically). We will call these states *isolated states*, as they are not coupled to any other loop configuration by the Hamiltonian.

We therefore find that the ground space degeneracy of H is at least *exponential* in N_v and N_h , and thus cannot be parametrized by strings of symmetry operations alone. In fact, e.g., the states

$$|v(0101)\rangle = \begin{array}{|c|c|c|c|} \hline \text{---} & \text{---} & \text{---} & \text{---} \\ \hline \text{---} & \text{---} & \text{---} & \text{---} \\ \hline \text{---} & \text{---} & \text{---} & \text{---} \\ \hline \text{---} & \text{---} & \text{---} & \text{---} \\ \hline \end{array}, \quad |v(1010)\rangle = \begin{array}{|c|c|c|c|} \hline \text{---} & \text{---} & \text{---} & \text{---} \\ \hline \text{---} & \text{---} & \text{---} & \text{---} \\ \hline \text{---} & \text{---} & \text{---} & \text{---} \\ \hline \text{---} & \text{---} & \text{---} & \text{---} \\ \hline \end{array} \quad (51)$$

are indistinguishable by any such string operation. It is worth pointing out, however, that all of these ground states are isolated and in the sector with maximal winding number, so it might still be possible that in the remaining sectors, the ground space can be parametrized succinctly in terms of the symmetry.

IV. CONCLUSIONS AND OUTLOOK

In this paper, we have studied PEPS with continuous virtual symmetries. Specifically, we have considered the class of $SU(2)$ -invariant PEPS with the fundamental representation of $SU(2)$, and studied their entanglement properties and their relation to local Hamiltonians. First, we have introduced the most general form of tensors invariant under the fundamental representation of $SU(2)$. From the local tensor, we have constructed local parent Hamiltonians acting on 2×2 sites, and characterized their ground space structure. For open boundaries, we have found that the ground space on rectangular patches on any size is always exactly parameterized by the PEPS, a property known as the intersection property. We were

further able to show that by choosing appropriate Hamiltonian terms at the boundary, the system acquires a unique ground state. On a system with periodic boundary conditions, we have found a ground space degeneracy which grows with the system size. We were able to attribute this to at least two distinct mechanisms: first, closing the boundaries with symmetry twists of $SU(2)$, in analogy to finite symmetry groups, yields a linearly growing number of ground states; and second, extremal isolated spin configurations yield an exponentially growing number of states. Regarding the entanglement properties of the state, we found that the zero Renyi entropy has a logarithmic correction to the area law scaling.

The observed results are clearly distinct from those found for known topologically ordered phases, and point towards a critical nature of the wave function (due to the logarithmic correction to the entanglement entropy and the algebraic ground space degeneracy, if the isolated states are ignored), or possibly some other exotic phase. Interestingly, for $\lambda = 1$ and an orthogonal physical site basis, $\langle 0|1\rangle_p = 0$, the normalization of the loop model corresponding to the $SU(2)$ -invariant PEPS can be mapped to the partition function of the $Q = 16$ state Potts model at the phase transition between ordered and disordered phase (see Appendix E), which is known to be a first-order transition with a finite correlation length; however, the mapping implies exponential decay of diagonal observables only. It may still be the case that other observables exhibit critical correlations (as is the case for the plaquette-flip for a related quantum loop model [21]). Thus, further studies might be required to determine the precise nature of the wave functions considered, and the way in which it is affected by the choice of λ and the local basis.

An interesting observation is that, for periodic boundaries and $\lambda = 1$, we obtain exactly the wave function of a quantum loop model $|\psi_{N_h \times N_v}(A, \text{PBC})\rangle = \sum_L d^{n_L} |L\rangle$, which was studied in Refs. [22,23]. The main focus of those works is the case where the so-called *topological weight* is $d = 2 \cos(\frac{\pi}{k+2}) < 2$ for k a positive integer. In that case, a Hamiltonian with a finite number of ground states on the torus in the thermodynamic limit can be found, in contrast to the exponential degeneracy we find in our model. The topological weight in our PEPS wave function is given by the bond dimension $d = 2$. While our construction can be extended to any integer $d > 2$, it is unclear whether a PEPS description with constant bond dimension exists for the quantum loop models investigated in the above references.

Finally, let us briefly comment on the significance of our findings with respect to numerical investigation of both loop models and other PEPS with continuous symmetries. First, in our model, when computing diagonal observables, the PEPS contraction coincides with the result of a Monte Carlo simulation [24]. This might indicate that PEPS with continuous symmetries beyond this model are susceptible to Monte Carlo schemes, and replacing the computationally heavy PEPS contraction in such a manner may prove useful, e.g., in variational calculations. Second, the existence of a virtual symmetry enables the use of quantum numbers. For example, the PEPS transfer matrix inherits the full $SU(2)$ symmetry of our tensor and one can attempt to find fixed points within each spin sector separately, thereby speeding up the computation.

ACKNOWLEDGMENTS

We are grateful for illuminating discussions with P. Fendley, F. Pollmann, and R. Verresen. We acknowledge the hospitality of the Centro de Ciencias de Benasque Pedro Pascual where part of the work was done. This work was supported by the European Research Council (ERC) under the European Union's Horizon 2020 research and innovation programme through the grants WASCOSYS (No. 636201) and QUENOCOBA (No. 742102).

APPENDIX A: ALLOWED CONNECTIVITY PATTERNS AND THE CANONICAL LOOP PATTERN

Both the degeneracy of the parent Hamiltonian and the entanglement entropy depends on the number $\mathcal{N}(N_h, N_v)$, i.e., the number of connectivity patterns on an $N_h \times N_v$ patch, which have at least one compatible loop pattern. In order to show that this number is equal to $\mathcal{N}(N_h, N_v) \sim \frac{4^N}{N^{3/2}}$ in Appendix B, we need to introduce the following terminology:

Definition: lattice and boundary. Define

$$\begin{aligned} \mathcal{X} &:= \left\{ \frac{1}{2}, \frac{3}{2}, \dots, \frac{2N_h - 1}{2} \right\} \times \{0, 1, \dots, N_v\}, \\ \mathcal{Y} &:= \{0, 1, \dots, N_h\} \times \left\{ \frac{1}{2}, \frac{3}{2}, \dots, \frac{2N_v - 1}{2} \right\}. \end{aligned} \quad (\text{A1})$$

The (N_h, N_v) lattice is defined as

$$\mathcal{L}_{N_h, N_v} = \mathcal{X} \cup \mathcal{Y}. \quad (\text{A2})$$

The *boundary* $\mathcal{B}_{N_h, N_v} \subset \mathcal{L}_{N_h, N_v}$ is

$$\mathcal{B}_{N_h, N_v} = \{(x, y) \in \mathcal{L}_{N_h, N_v} \mid x \in \{0, N_h\} \text{ or } y \in \{0, N_v\}\}. \quad (\text{A3})$$

Definition: tuple distance. Let $a, b \in \mathcal{L}_{N_h, N_v}$, $a \neq b$ and writing $a = (a_x, a_y)$, $b = (b_x, b_y)$, the x distance (y distance) of the tuple (a, b) is

$$\Delta x(a, b) = b_x - a_x, \quad \Delta y(a, b) = b_y - a_y. \quad (\text{A4})$$

A tuple (a, b) is

$$\begin{aligned} &\text{horizontal if } |\Delta x(a, b)| > |\Delta y(a, b)|, \\ &\text{vertical if } |\Delta x(a, b)| < |\Delta y(a, b)|, \quad \text{and} \\ &\text{diagonal if } |\Delta x(a, b)| = |\Delta y(a, b)|. \end{aligned} \quad (\text{A5})$$

A horizontal tuple (a, b) is *upper* if $a_y + b_y \leq N_v$, otherwise it is *lower*. A vertical tuple (a, b) is *left* if $a_x + b_x \leq N_h$, otherwise it is *right*.

In the main text, we define allowed and forbidden matchings by the existence of at least one compatible loop pattern. We will now give a more useful definition in terms of *Flow* and then show that the definitions are equivalent, i.e., show that for each allowed connectivity pattern as defined here there exists at least one loop pattern: the canonical loop pattern. The fact that there cannot exist a loop pattern for forbidden matchings is easy to see.

Definition: Flow. For $i \in \{1, N_h - 1\}$ ($i \in \{1, N_v - 1\}$) and $a, b \in \mathcal{L}_{N_h, N_v}$, the tuple (a, b) goes through vertical

(horizontal) cut i if (a, b) is horizontal (vertical) and

$$\begin{aligned} &a_x < i \quad \text{and} \quad b_x > i \\ &(a_y < i \quad \text{and} \quad b_y > i). \end{aligned} \quad (\text{A6})$$

For p , a connectivity pattern, the *flow through vertical (horizontal) cut i* , denoted by $Flow(p, i, vert)$ ($Flow(p, i, hor)$) is the number of bonds $t \in p$ that go through vertical (horizontal) cut i .

Definition: forbidden matchings. We call a connectivity pattern p *vertically forbidden* if there exists $i \in \{1, 2, \dots, N_h - 1\}$ such that

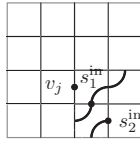
$$Flow(p, i, vert) \geq N_v + 1 \quad (\text{A7})$$

or *horizontally forbidden* if there exists $i \in \{1, 2, \dots, N_v - 1\}$ such that

$$Flow(p, i, hor) \geq N_h + 1. \quad (\text{A8})$$

A connectivity pattern that is not forbidden is *allowed*.

Definition: the canonical loop pattern. Given an allowed connectivity pattern $p = \{(a_1, b_1), \dots, (a_N, b_N)\}$, we construct the loop pattern explicitly. (1) We start with the empty loop pattern $L = \{\}$. (2) (*Initial and final pieces.*) For each $t_i = (a_i, b_i)$, determine whether it is horizontal, diagonal, or vertical. If t_i is horizontal or diagonal and $a_i(b_i) \in \mathcal{X}$ then define $\bar{a}_i = a_i + (1/2, \pm 1/2)$ and $\bar{b}_i = b_i + (-1/2, \pm 1/2)$, depending on whether $a_i(b_i)$ are located on the top or bottom boundary. Similarly, if t_i is vertical and $a_i(b_i) \in \mathcal{Y}$, define $\bar{a}_i = a_i + (\pm 1/2, 1/2)$ and $\bar{b}_i = b_i + (\pm 1/2, -1/2)$. Else, just set $\bar{a}_i = a_i$ and $\bar{b}_i = b_i$. This causes all horizontal and diagonal bonds effectively go from \mathcal{X} to \mathcal{Y} and all vertical bonds to go from \mathcal{Y} to \mathcal{X} . (3) (*Choosing a bond.*) Pick a bond $t = (a, b) \in p$, such that all bonds inside t have been picked already. Since two paths cannot be mutually inside each other, there always exists such a path, except if all bonds have been chosen. In that case, continue with step 8. Define a new partial path $m = \{(a), \bar{a}\}$ (the brackets indicate to only add a if $a \neq \bar{a}$). (4) Set $j = 1$ and $v_1 = \bar{a}$. (5) If $v_j = \bar{b}$, add the completed path $m = \{(a), \bar{a}, v_2, \dots, \bar{b}, (b)\}$ to L and go back to step 3. Otherwise continue with the step 6. (6) (*Diagonal partial paths.*) If the pair (v_j, \bar{b}) is diagonal, consider without loss of generality the case where $x(\bar{b}) > x(v_j)$ and $y(\bar{b}) > y(v_j)$. Then, set $v_{j+1} = v_j + (1/2, 1/2)$. In the other cases, extend the path towards \bar{b} analogously. In principle, v_{j+1} could already be occupied by a path q . However, as will become clear in the next step, all paths are constructed *monotonously*, i.e., horizontal paths advance towards the right in each step and vertical paths advance towards the bottom. Therefore one can draw a horizontal (vertical) cone if q is horizontal (vertical) and the endpoints, let's call them a_q and b_q , must lie inside the cone as well, one to the right (top) of v_{j+1} and one to the left (bottom). It is easy to see that the bonds (a_q, b_q) and (a, b) are crossing, violating the assumption that m is a valid matching. Add v_{j+1} to p , set $j \leftarrow j + 1$ and go back to step 5. (7) (*All other types of partial paths.*) If (v_j, \bar{b}) is not diagonal, consider without loss of generality (a, b) to be a lower horizontal bond (all other cases follow analogously). By construction (see below), at any


 FIG. 2. s_1^{in} touching the boundary.

point, (v_j, \bar{b}) remains horizontal. Define

$$\begin{aligned} s_1^{\text{in}} &= v_j + (1/2, 1/2), \\ s_1^{\text{out}} &= v_j + (1/2, -1/2), \\ s_2^{\text{in}} &= s_1^{\text{in}} + (1/2, 1/2), \\ s_2^{\text{out}} &= s_1^{\text{out}} + (1/2, -1/2). \end{aligned} \quad (\text{A9})$$

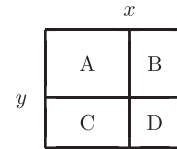
If neither of s_1^{in} and s_2^{in} is occupied or in the boundary, set $v_{j+1} = s_1^{\text{in}}$ and $v_{j+2} = s_2^{\text{in}}$. Otherwise, set $v_{j+1} = s_1^{\text{out}}$ and $v_{j+2} = s_2^{\text{out}}$. Add v_{j+1} and v_{j+2} to p , set $j \leftarrow j + 1$ and go back to step 5.

Again, in principle, one of s_1^{in} and s_2^{in} and one of s_1^{out} and s_2^{out} could be occupied or in the boundary. We are now going to show that in this case p is forbidden, i.e., there is too much flow going through a horizontal/vertical line. First, let us assume that s_2^{in} is occupied. Denote by q the path that contains s_2^{in} and call its endpoints (a_q, b_q) . Then q must be horizontal, which can be verified using the fact that (v_j, b) is horizontal. As such, $v_j + (1/2, 3/2) \in q$, since v_j is still free. Now we have two horizontal paths, p and q , both go through $x(v_j)$ and their vertical distance at that point is 2. By construction, the vertical distance must remain even all the way through to the initial and final points of paths q and m , which implies that there is an odd number of boundary points between a_m and a_q and between b_m and b_q . Hence there is one horizontal bond (a_r, b_r) that goes through $x(s_2^{\text{in}})$ and (a_q, b_q) lies inside it.

Consider now $s_1^{\text{in}'} = s_1^{\text{in}} + (0, 1)$ and $s_2^{\text{in}'} = s_2^{\text{in}} + (0, 1)$. If either of them are in the boundary, the situation is depicted in Fig. 2. Otherwise, consider the progression from $v_j + (1/2, 3/2)$ to $s_2^{\text{in}'}$: it is an up-move and it is occurring in a lower horizontal path. Hence either of $s_1^{\text{in}'}$ or $s_2^{\text{in}'}$ must be occupied. If $s_2^{\text{in}'}$ is occupied, the above argument can be repeated until one reaches the boundary to find $N_v - y(v_j) + 1/2$ horizontal bonds that go through $x(s_2^{\text{in}'})$. If $s_1^{\text{in}'}$ is occupied, its path must be horizontal and running parallel to q , in particular making an up-step around $s_1^{\text{in}'}$. Again, we can continue the argument until we arrive at the boundary. The same argument can be used if initially s_1^{in} is occupied instead of s_2^{in} . In either case, we find $N_v - y(v_j) + 1/2$ horizontal bonds that go through $x(s_2^{\text{in}'})$.

Now, by assumption, also either s_1^{out} or s_2^{out} is occupied. We can reverse top and bottom in the argument above to find another $y(v_j) + 1/2$ horizontal bonds which go through $x(s_2^{\text{in}'})$. Note that the path that contains s_2^{out} is necessarily upper, since otherwise, m would be inside it and it could not exist yet by construction.

We have hence found $N_v + 1$ bonds in p that go through a single vertical cut, contradicting the assumption that p is allowed. (8) (*Adding bubbles*) Now for each bond, we have created a connecting path. It is possible, however, that not all points in \mathcal{L}_{N_h, N_v} are occupied. In this case, we add small bubbles to the pattern.


 FIG. 3. The boundary cut into regions by vertical and horizontal cuts at x and y .

It remains to show that the loop pattern thus created is compatible with p , i.e., that the boundary points of all paths correspond to tuples in the connectivity pattern, or—differently phrased—for a tuple $(a, b) \in p$, whether the corresponding path in L starting with a can end at a point $b' \neq b$. By construction, once (v_j, b) becomes diagonal, it will surely have the correct ending point. Again, let us consider without loss of generality a horizontal path. Then, after Δx steps, the horizontal distance to the target is zero. Hence, either we have arrived at the correct ending point, or the partial path has become vertical during the construction. To become vertical, however, the path must have gone through a point where its remainder was diagonal, hence ensuring that the correct ending point was reached. The resulting loop pattern is the *canonical loop pattern of p* .

APPENDIX B: THE NUMBER $\mathcal{N}(N_h, N_v)$

Now that we have seen that there is at least one loop pattern for each allowed connectivity pattern, we can count the forbidden connectivity patterns.

1. We can count horizontally and vertically forbidden connectivity patterns individually

Claim. A connectivity pattern cannot be both horizontally and vertically forbidden.

Proof. Let p be a connectivity pattern and assume it is both horizontally and vertically forbidden. Then denote the vertical lines at which there is an oversaturated cut by x and y , respectively. These lines cut the patch into four areas, A , B , C , and D as depicted in Fig. 3.

Now if each of the bonds cuts only either the horizontal or vertical line, then there would need to be at least $N_h + N_v + 2$ bonds in total, hence at least two bonds cut both lines, without loss of generality going from boundary A to boundary D in the figure. There could be more than two bonds crossing from A to D —let us denote the total number by κ , the lowest one by a and the highest one by b . These bonds partition the areas A and D into A_L, A_R and D_L, D_R , respectively. For their size, clearly

$$|A_L| + |A_R| + \kappa \leq |A|, \quad |D_L| + |D_R| + \kappa \leq |D| \quad (\text{B1})$$

holds. There remain $N_h - \kappa + 1$ bonds to be found for the horizontal violation and all of these must have boundary points in A_R and D_R . Similarly, there remain $N_v - \kappa + 1$ bonds to be found for the vertical violation and all of these must have boundary points in A_L and D_L . Hence we have the inequalities

$$\begin{aligned} |A_L| + |D_L| &\geq N_v - \kappa + 1, \\ |A_R| + |D_R| &\geq N_h - \kappa + 1. \end{aligned} \quad (\text{B2})$$

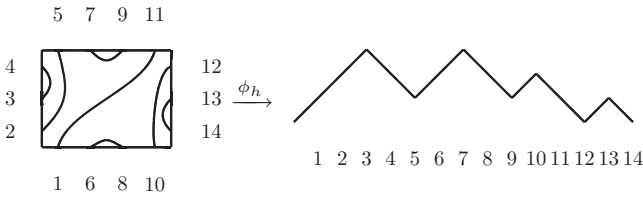


FIG. 4. The mapping ϕ_h for an allowed connectivity pattern.

Adding the two inequalities and inserting inequalities (B1), we obtain

$$|A| + |D| \geq N_v + N_h + 2, \tag{B3}$$

and since $|A| + |D| = N_v + N_h$, we arrive at a contradiction. ■

2. A bijection between connectivity patterns and Dyck paths

Definition: Dyck paths. A Dyck path or mountain diagram of size n is a lattice path in \mathbb{Z}^2 from $(0,0)$ to $(2n, 0)$ consisting of n up steps of the form $(1,1)$ and n down steps of the form $(1, -1)$, which never goes below the x axis $y = 0$. The maximal height of a Dyck path is the maximum y coordinate of the path. Denote all Dyck paths of size n by \mathcal{D}_n .

Definition: Bijection between connectivity patterns and Dyck paths. We define two maps

$$\begin{aligned} \phi_h : (N_h, N_v)\text{-connectivity patterns} &\mapsto \mathcal{D}_{N_h+N_v}, \\ \phi_v : (N_h, N_v)\text{-connectivity patterns} &\mapsto \mathcal{D}_{N_h+N_v}. \end{aligned} \tag{B4}$$

The image of a given connectivity pattern p under the map ϕ_h is given as follows. We start with the empty Dyck path and sequentially look at the boundary points in the order given in Fig. 4. Then, we add an up-step to the Dyck path if the partner of the boundary point we are currently reading has not been read yet. Otherwise, we add a down-step. For ϕ_v , we follow the same procedure with the labeling given by Fig. 5 instead.

A couple of remarks are in order. (1) The resulting path is a Dyck path: for it to pierce through the x axis, one would need to read more second halves than first halves up to a given point, which is clearly impossible. Also, there is an equal number of second halves and first halves in total, so the final step ends up on the x axis again. (2) The maps ϕ_h and ϕ_v are bijective. The map ϕ_h^{-1} reads the Dyck path sequentially from start to end, while scanning through the boundary points in the order given in Fig. 4. Whenever a down-step is encountered, a bond is added to the connectivity pattern by matching the currently active boundary point with the last open one. Again, ϕ_v^{-1} works analogously with the labeling given in Fig. 5. (3) For $i \in \{1, 2, \dots, N_h - 1\}$, $Flow(p, i, vert)$ is given

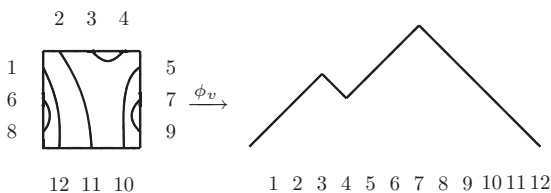


FIG. 5. The mapping ϕ_v for a forbidden connectivity pattern.

by the height of $\phi_h(p)$ after $N_v + 2i$ steps. Similarly, for $j \in \{1, 2, \dots, N_v - 1\}$, $Flow(p, j, hor)$ is given by the height of $\phi_v(p)$ after $N_h + 2i$ steps. In particular, p is horizontally (vertically) forbidden if the maximal height of $\phi_h(p)$ ($\phi_v(p)$) is greater than N_h (N_v).

3. Three expressions for the number of Dyck paths with restricted height

Claim (number of allowed matchings). Let $C_n = \frac{1}{n+1} \binom{2n}{n}$ be the regular Catalan number. For a given $N_h, N_v \in \mathbb{N}$, the number of horizontally (vertically) forbidden connectivity pattern is given by $C_{N_h+N_v} - f(N_h, N_v)$ ($C_{N_h+N_v} - f(N_v, N_h)$), where we can give three expressions for the numbers $f(N_h, N_v)$:

$$\begin{aligned} f(N_h, N_v) &= \frac{4^N}{1 + \frac{N_h}{2}} \sum_{j=1}^{N_h+2} \sin\left(\frac{\pi j}{N_h+2}\right) \left(\cos\left(\frac{\pi j}{N_h+2}\right)\right)^{2N} \\ &= \sum_{k \geq 1} \binom{2N}{N - k(N_h + 2) - 1} \\ &\quad - 2 \binom{2N}{N - k(N_h + 2)} + \binom{2N}{N - k(N_h + 2) + 1} \\ &= \left(\frac{d}{dz}\right) \Big|_{z=0} \frac{1}{1 - \frac{z^2}{\dots - \frac{1}{z^2}}}, \end{aligned} \tag{B5}$$

where the continued fraction has N_h instances of z^2 and $N = N_h + N_v$. As a direct corollary, since forbidden matchings are either horizontally or vertically forbidden and the number of all matchings is $C_{N_h+N_v}$, we obtain the total number of allowed matchings:

$$\mathcal{N}(N_h, N_v) = f(N_h, N_v) + f(N_v, N_h) - C_{N_h+N_v}. \tag{B6}$$

For later convenience, we will introduce $f(N_h, \alpha)$, with the aspect ratio $\alpha N_v = N = N_h + N_v$. Since the number of vertically forbidden matchings is equal to the number of horizontally forbidden matchings on a 90° rotated patch and a 90° rotation corresponds to $\alpha \rightarrow \frac{\alpha}{\alpha-1}$, we can rewrite Eq. (B6) as

$$\mathcal{N}(N_h, \alpha) = f(N_h, \alpha) + f\left(N_h, \frac{\alpha}{\alpha-1}\right) - C_{\alpha N_h}. \tag{B7}$$

Proof. Let $N_h, N_v \in \mathbb{N}$. We are going to count the horizontally allowed connectivity pattern and show that they are equal to $C_{N_h+N_v} - f(N_h, N_v)$. From the definition of Dyck paths, we need to count all mountain diagrams of half-length $N_h + N_v$ whose maximum height exceeds N_h . To this end, we set up a sequence of counting vectors $v_i \in \mathbb{N}^{N_h+1}$. After n steps, we would like the number of paths with height h that never exceed N_h in height to be given by $(v_n)_h$. Hence, set $v_0 = (1, 0, \dots, 0)$, indicating a single path with height 0, the empty path. Now we

the sine and finally, we replace the sum by an integral that we can compute analytically. All of these approximations induce an error $\mathcal{O}(1/N)$.

Let us now establish the relevant claims.

Definition.

$$e_1(N) := \sqrt{N} \sum_{j=\lfloor N/\pi \rfloor}^{N/2} \sin^2\left(\frac{\pi j}{N}\right) \cos^{2\alpha N}\left(\frac{\pi j}{N}\right). \quad (\text{B20})$$

Claim. Truncation of the sum.

$$e_1(N) = \mathcal{O}(N^{3/2}2^{-\alpha N}). \quad (\text{B21})$$

Proof. For j in the interval $[\lfloor N/\pi \rfloor, N/2]$, for N large enough we have that $j\pi/N \geq \pi/4$ and therefore

$$\begin{aligned} e_1(N) &\leq \sqrt{N} \sum_{j=\lfloor N/\pi \rfloor}^{N/2} \sin^2\left(\frac{\pi j}{N}\right) \cos^{2\alpha N}(\pi/4) \\ &= \sqrt{N} \sum_{j=\lfloor N/\pi \rfloor}^{N/2} \sin^2\left(\frac{\pi j}{N}\right) 2^{-\alpha N} \\ &\leq N^{3/2}2^{-\alpha N}. \end{aligned} \quad (\text{B22})$$

Definition.

$$e_2(N) := \sqrt{N} \sum_{j=1}^{\lfloor N/\pi \rfloor} \sin^2\left(\frac{\pi j}{N}\right) \left[e^{-\alpha N(\frac{\pi j}{N})^2} - \cos^{2\alpha N}\left(\frac{\pi j}{N}\right) \right] \quad (\text{B23})$$

Claim. A cosine raised to a high power becomes a Gaussian.

$$e_2(N) = \mathcal{O}\left(\frac{1}{N}\right). \quad (\text{B24})$$

Proof. For simplicity, define $x_j = \frac{\pi j}{N}$ and $M = 2\alpha N$. Using $\cos(x) \geq 1 - \frac{1}{2}x^2 > 0$ in the interval $x \in [0, 1]$ and the fact that each term in the sum is positive, we have

$$\begin{aligned} e_2(N) &\leq \sqrt{N} \sum_{j=1}^{\lfloor N/\pi \rfloor} \sin^2(x_j) \left[e^{-\frac{x_j^2}{2}M} - \left(1 - \frac{1}{2}x_j^2\right)^M \right] \\ &= \sqrt{N} \sum_{j=1}^{\lfloor N/\pi \rfloor} \sin^2(x_j) \left[e^{-\frac{x_j^2}{2}M} - \left(1 - \frac{\frac{1}{2}x_j^2 M}{M}\right)^M \right]. \end{aligned} \quad (\text{B25})$$

Since $\frac{1}{2}x_j^2 < 1$, we can use the inequality $(1 - \frac{1}{2}x_j^2 M)^M \geq e^{-\frac{x_j^2}{2}M(1 - \frac{1}{2}x_j^2)}$, combined with $0 < \sin(x_j) < x_j$ and $e^{-y} \geq 1 - y$ to arrive at

$$\begin{aligned} e_2(N) &\leq \sqrt{N} \sum_{j=1}^{\lfloor N/\pi \rfloor} x_j^2 \left[e^{-\frac{x_j^2}{2}M} - e^{-\frac{x_j^2}{2}M \frac{1 - \frac{1}{2}x_j^2}{1 - \frac{x_j^2}{2}}} \right] \\ &= \sqrt{N} \sum_{j=1}^{\lfloor N/\pi \rfloor} x_j^2 e^{-\frac{x_j^2}{2}M} \left[1 - e^{\frac{x_j^2}{2}M(1 - \frac{1}{2}x_j^2)} \right] \end{aligned}$$

$$\begin{aligned} &\leq \sqrt{N} \sum_{j=1}^{\lfloor N/\pi \rfloor} x_j^2 e^{-\frac{x_j^2}{2}M} \left(-\frac{x_j^2}{2} M \left(1 - \frac{1}{1 - \frac{x_j^2}{2}} \right) \right) \\ &\leq \frac{\sqrt{N}M}{2} \sum_{j=1}^{\lfloor N/\pi \rfloor} x_j^6 e^{-\frac{x_j^2}{2}M} \underbrace{\frac{1}{1 - \frac{x_j^2}{2}}}_{\leq 2} \\ &\leq N^{5/2} \frac{2\alpha}{\pi} \frac{1}{\lfloor N/\pi \rfloor} \sum_{j=1}^{\lfloor N/\pi \rfloor} x_j^6 e^{-\frac{x_j^2}{2}M}. \end{aligned} \quad (\text{B26})$$

The sum is the right Riemann sum of the function $f(x) = \pi^2 x^6 e^{-x^2 \alpha N \pi^2}$, with an error given by

$$\left| \frac{1}{\lfloor N/\pi \rfloor} \sum_{j=1}^{\lfloor N/\pi \rfloor} x_j^6 e^{-\frac{x_j^2}{2}M} - \int_0^1 \pi^2 x^6 e^{-x^2 \alpha N \pi^2} dx \right| \leq \frac{d_{\max}}{2\lfloor N/\pi \rfloor}, \quad (\text{B27})$$

where d_{\max} is the maximum of the derivative $f'(x)$ in the interval $[0, 1]$. A direct calculation reveals that

$$d_{\max} = c(N\alpha)^{-5/2} \quad (\text{B28})$$

for some constant c . Plugging (B28) and (B27) into (B26) yields

$$\begin{aligned} e_2(N) &= N^{5/2} 2\alpha \pi \int_0^1 x^6 e^{-x^2 \alpha N} dx + \mathcal{O}\left(\frac{1}{N}\right) \\ &\leq N^{5/2} 2\alpha \pi \int_0^\infty x^6 e^{-x^2 \alpha N} dx + \mathcal{O}\left(\frac{1}{N}\right) \\ &= N^{5/2} 2\alpha \pi \frac{15\sqrt{\pi}}{16} (N\alpha\pi^2)^{-7/2} + \mathcal{O}\left(\frac{1}{N}\right) \\ &= \mathcal{O}\left(\frac{1}{N}\right). \end{aligned} \quad (\text{B29})$$

Definition.

$$e_3(N) := \sqrt{N} \sum_{j=1}^{\lfloor N/\pi \rfloor} e^{-\alpha N(\frac{\pi j}{N})^2} \left[\sin^2\left(\frac{\pi j}{N}\right) - \left(\frac{\pi j}{N}\right)^2 \right]. \quad (\text{B30})$$

Claim. Replacing the sine.

$$e_3(N) := \mathcal{O}\left(\frac{1}{N}\right). \quad (\text{B31})$$

Proof. Taylor expanding the sine yields

$$\sin^2(x) = x^2 - \frac{1}{3} \cos(2\xi) x^4 \quad (\text{B32})$$

for some $\xi \in [0, x]$. Plugging (B32) into (B30) and using a Riemann sum bound akin to (B27) leads to

$$\begin{aligned} e_3(N) &\leq \sqrt{N} \sum_{j=1}^{\lfloor N/\pi \rfloor} e^{-\alpha N(\frac{\pi j}{N})^2} \left(\frac{\pi j}{N}\right)^4 \\ &\leq N^{3/2} \pi^2 \int_0^1 x^4 e^{-\alpha N x^2 \pi^2} dx \end{aligned}$$

$$\begin{aligned}
 &\leq N^{3/2}\pi^2 \int_0^\infty x^4 e^{-\alpha N x^2 \pi^2} dx \\
 &\leq N^{3/2}\pi^2 \frac{3}{8} \sqrt{\pi} (\alpha \pi^2 N)^{-5/2} \\
 &= \mathcal{O}\left(\frac{1}{N}\right). \tag{B33}
 \end{aligned}$$

Definition. ■

$$r(N) := \sqrt{N} \sum_{j=1}^{\lfloor N/\pi \rfloor} x_j^2 e^{-\alpha N x_j^2} \tag{B34}$$

Claim. Computation of the integral.

$$r(N) := \frac{\sqrt{\pi}}{4\alpha^{3/2}} + \mathcal{O}\left(\frac{1}{N}\right). \tag{B35}$$

Proof. The usual bound for the Riemann sum (B27) implies

$$\begin{aligned}
 r(N) &= \sqrt{N} \lfloor N/\pi \rfloor \frac{1}{\lfloor N/\pi \rfloor} \sum_{j=1}^{\lfloor N/\pi \rfloor} x_j^2 e^{-\alpha N x_j^2} \\
 &= \sqrt{N} \lfloor N/\pi \rfloor \pi^2 \int_0^1 x^2 e^{-\alpha N x^2 \pi^2} dx + \mathcal{O}\left(\frac{1}{N}\right). \tag{B36}
 \end{aligned}$$

We can extend the integral to infinity by noting that $x^2 \leq x e^{x^2}$:

$$\begin{aligned}
 \int_1^\infty x^2 e^{-\alpha N x^2} dx &\leq \int_1^\infty x e^{1-\alpha N x^2} \\
 &= \frac{e^{-\alpha N + 1}}{2(\alpha N - 1)} \\
 &= \mathcal{O}(e^{-N}), \tag{B37}
 \end{aligned}$$

implying that

$$\begin{aligned}
 r(N) &= \sqrt{N} \lfloor N/\pi \rfloor \pi^2 \int_0^\infty x^2 e^{-\alpha N x^2 \pi^2} dx + \mathcal{O}\left(\frac{1}{N}\right) \\
 &= \sqrt{N} \lfloor N/\pi \rfloor \pi^2 \frac{\sqrt{\pi}}{4(\alpha N \pi^2)^{3/2}} + \mathcal{O}\left(\frac{1}{N}\right) \\
 &= \frac{\sqrt{\pi}}{4\alpha^{3/2}} + \mathcal{O}\left(\frac{1}{N}\right). \tag{B38}
 \end{aligned}$$

Corollary 1. ■

$$g(N_h, \alpha) = \frac{\sqrt{\pi}}{2\alpha^{3/2}} + \mathcal{O}\left(\frac{1}{N_h}\right). \tag{B39}$$

Proof. This follows directly from the four previous claims. ■

Corollary 2.

$$\mathcal{N}(\alpha, N) = \frac{4^N}{N^{3/2}} \left[k(\alpha) + \mathcal{O}\left(\frac{1}{N}\right) \right]. \tag{B40}$$

Proof. For large N , we have

$$\begin{aligned}
 \mathcal{N}(\alpha, N) &= 4^N \left[N_h^{-3/2} g(N_h, \alpha) \right. \\
 &\quad \left. + N_h^{-3/2} g\left(N_h, \frac{\alpha}{\alpha-1}\right) - N^{-3/2} \pi^{-1/2} \right] \\
 &= 4^N \left[N_h^{-3/2} \frac{\sqrt{\pi}}{2\alpha^{3/2}} \right. \\
 &\quad \left. + N_h^{-3/2} \frac{\sqrt{\pi}}{2\frac{\alpha}{\alpha-1}^{3/2}} - N^{-3/2} \pi^{-1/2} \right] \\
 &= \frac{4^N}{N^{3/2}} \left[\frac{\sqrt{\pi}}{2} + \frac{\sqrt{\pi}}{2} (\alpha-1)^{3/2} \right. \\
 &\quad \left. - \pi^{-1/2} + \mathcal{O}\left(\frac{1}{N}\right) \right]. \tag{B41}
 \end{aligned}$$

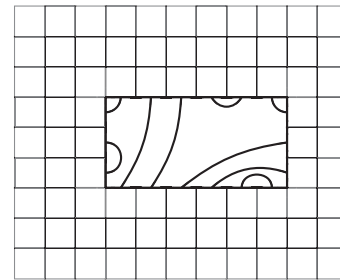
■

APPENDIX C: THE MATRIX Ψ_R IN (25) IS INVERTIBLE

The matrix $\Psi_R : V_{\text{matchings}} \mapsto V_{\text{loops}}^B$ maps connectivity patterns on the boundary of a hole *inside* the torus onto loop patterns on the complement of the hole. *A priori*, this map does not have to be invertible. We show here that for a torus much larger than the hole, Ψ_R is invertible. More precisely, if the size of the rectangular hole is $L_h \times L_v$ and the torus is $N_h \times N_v$, then we require

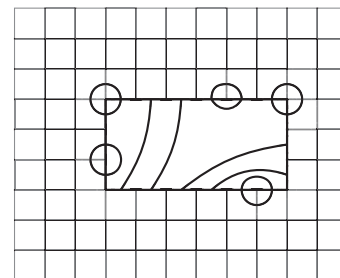
$$\min\{N_h, N_v\} > \frac{3}{2}(L_h + L_v). \tag{C1}$$

The kernel of Ψ_R is nonempty if and only if for every connectivity pattern, there exists a loop pattern on R that is compatible with it. The following procedure produces such a loop pattern for an arbitrary inside connectivity pattern.



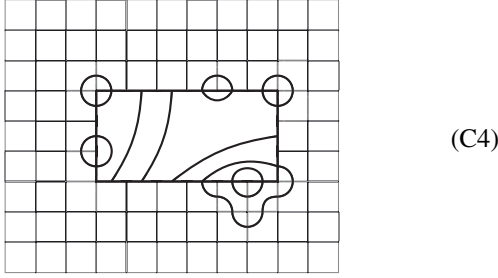
(C2)

Since we work on the torus, we can draw the rectangle in the center of our lattice. (1) Close any nearest neighbours in a minimal way (as shown in the figures). Clearly, these cannot interfere with each other. This can be done within one tile from the hole.

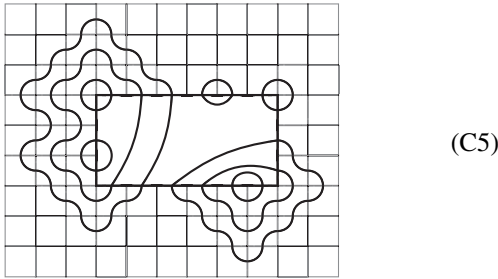


(C3)

(2) Remove the connected pairs from the connectivity pattern. There must necessarily be at least one newly formed nearest-neighbor pair. Connect these minimally, avoiding the bonds that are already closed. This can be done within two tiles from the hole.



(3) Again remove the connected pairs from the connectivity pattern, creating new nearest neighbours. As long as there is enough space on the torus, these pairs can be closed minimally. For each nested bond, one more tile of space is needed.



(4) Fill the rest of the loop pattern arbitrarily. For a hole of size $L_h \times L_v$, there can be at most $\lceil \frac{L_h + L_v}{2} \rceil$ nested bonds. Therefore, if $\min\{N_h, N_v\} > \frac{3}{2}(L_h + L_v)$, then there is enough space in every direction for the above procedure to generate a compatible loop pattern.

APPENDIX D: UNIQUENESS OF THE GROUND STATE WITHIN A GIVEN CONNECTIVITY CLASS

Having defined the canonical loop pattern of a connectivity pattern, we can now prove that the Hamiltonian defined by (28) is ergodic in the sense that for every two loop patterns L and L' in the same connectivity class, there exists a sequence of surgery moves such that

$$L' = \sigma_M(\sigma_{M-1}(\dots \sigma_1(L)) \dots). \quad (\text{D1})$$

The algorithm to arrive at the canonical loop pattern from an arbitrary starting pattern from surgery moves only contains three steps. (1) Tadpoles and larger bubbles are cut off. (2) All paths are consecutively made as short as possible. Any path with nonminimal length must necessarily contain both vertical and horizontal *bay-type* plaquettes [Fig. 6(b)]. This pair must necessarily contain a loop in their inside. The loop can be moved through the bay by three consecutive surgery moves. If the bays had previously been adjacent, the path is now shorter, otherwise the bays are now closer together. Therefore any path can be made as short as possible. Note that any surgery move only acts on one path plus a surrounding loop so previously shortened paths will always stay shortest during the application of further elementary moves in this step. (3) Every path now

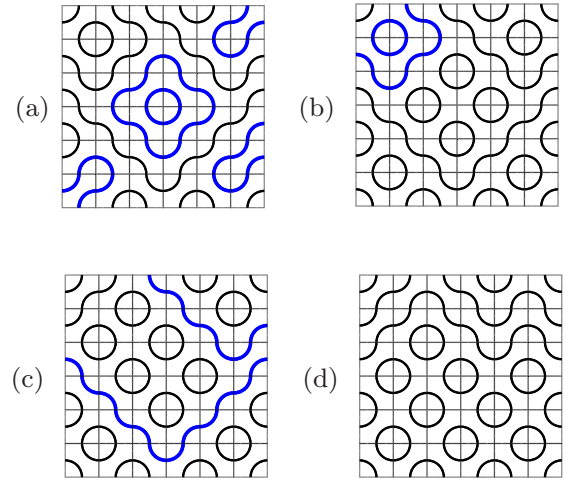


FIG. 6. Bringing a given loop pattern (a) into the canonical pattern with the same boundary matching (d). In step 1, tadpoles and larger bubbles are cut off into small bubbles (b). Every path is shortened as much as possible in step 2 (c). The remaining ambiguity is the trajectory of longer paths. For the sake of uniqueness, they are moved as close as possible to the north-west boundary (d).

exclusively consists of *up* and *down* moves, the order of which may still differ from the canonical loop pattern, i.e., the path might not run as close as possible to the north-west boundary of the patch [Fig. 6(c)]. For the pattern to be compatible with the same boundary matching, the area between the current and the desired trajectory for any given path must be filled with small bubbles. We are finished after moving all the bubbles through the appropriate bays.

APPENDIX E: MAPPING TO THE CLASSICAL DELTA POTTS MODEL

In this section, we will prove that certain correlation functions in the PEPS decay exponentially for $\lambda = 1$ (8), by establishing a mapping to an observable in a classical model. We will start out with the case $u = \langle 0|1 \rangle_p = 0$ and comment on the general case later on. For better readability, we denote the state at $\lambda = 1$, $u = 0$ on a torus of size $N_h \times N_v$ with both N_h and N_v even by

$$|\psi\rangle := |\psi_{N_h \times N_v}(u = 0, \lambda = 1)\rangle = \sum_{\text{loop patterns } L} 2^{n_L} |L\rangle. \quad (\text{E1})$$

Definition.

$$\tilde{\sigma}_z(\vec{x}) := \begin{cases} \sigma_z(\vec{x}) & \text{if } \vec{x} \text{ is on the even sublattice} \\ -\sigma_z(\vec{x}) & \text{if } \vec{x} \text{ is on the odd sublattice.} \end{cases} \quad (\text{E2})$$

A plaquette $\vec{x} = (x_1, x_2)$ is on the even (odd) sublattice if $x_1 + x_2$ is even (odd). The top left plaquette has coordinates (1,1).

$$C[\vec{x}, \vec{y}] := \frac{\langle \psi | \tilde{\sigma}_z(\vec{x}) \tilde{\sigma}_z(\vec{y}) | \psi \rangle}{\langle \psi | \psi \rangle} - \frac{\langle \psi | \tilde{\sigma}_z(\vec{x}) | \psi \rangle \langle \psi | \tilde{\sigma}_z(\vec{y}) | \psi \rangle}{\langle \psi | \psi \rangle^2}. \quad (\text{E3})$$

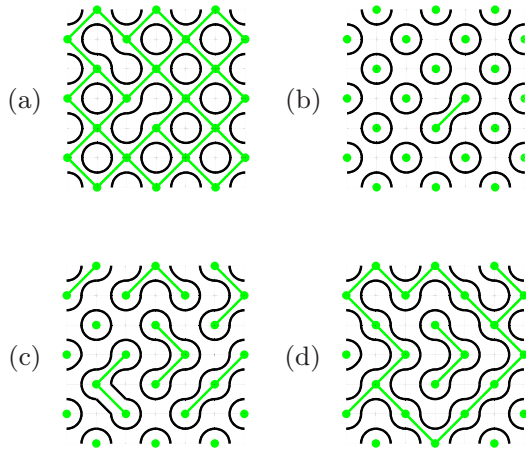


FIG. 7. Typical configurations in the Fortuin-Kasteleyn expansion of the partition function of the Potts model. The green lines correspond to the clusters in the expansion. Each cluster configuration is associated with a unique loop pattern. (a) A typical configuration of the Potts model in the ordered phase, (b) a typical configuration in the disordered phase, (c) the Potts model at the phase transition point for $Q > 4$, and (d) for values $Q \leq 4$. Only for the latter, loops of all length scales occur, whereas the bounded loop length in all other cases corresponds to a finite correlation length.

Claim.

$$C[\vec{x}, \vec{y}] \xrightarrow{|\vec{x}-\vec{y}| \rightarrow \infty} e^{-\frac{|\vec{x}-\vec{y}|}{\xi}} \quad (\text{E4})$$

for some $\xi > 0$.

Proof. Consider a classical Q -state Potts model with spins residing on the vertices of the *net lattice*. The net lattice is a square lattice rotated by 45° where the distance between the vertices is increased by a factor $\sqrt{2}$ (the vertices are marked with green dots in Fig. 7). The classical spins take values $\sigma \in \{1, \dots, Q\}$. The Hamiltonian of the model is given by

$$H = - \sum_{\langle ij \rangle} \delta(\sigma_i, \sigma_j), \quad (\text{E5})$$

where $\langle ij \rangle$ indicates nearest neighbors on the net lattice. For a plaquette of the original square lattice located at \vec{x} , define by \vec{x}_a and \vec{x}_b the two spins adjacent to that plaquette (the order will not matter for our purposes). Define the following ‘‘link’’ observable in the Potts model that acts on two spins:

$$O_{\vec{x}}(\{\sigma\}) := \begin{cases} 1 & \text{if } \sigma_{\vec{x}_a} = \sigma_{\vec{x}_b} \\ \frac{1+Q}{1-Q} & \text{if } \sigma_{\vec{x}_a} \neq \sigma_{\vec{x}_b} \end{cases}. \quad (\text{E6})$$

Consider the expectation value of $O_{\vec{x}}$ in such a Potts model at inverse temperature β :

$$\langle O_{\vec{x}} \rangle = \frac{1}{Z} \sum_{\{\sigma\}} O_{\vec{x}}(\{\sigma\}) \prod_{\langle ij \rangle} e^{-\beta \delta(\sigma_i, \sigma_j)} \quad (\text{E7})$$

$$= \frac{1}{Z} \sum_{\{\sigma\}} O_{\vec{x}}(\{\sigma\}) \prod_{\langle ij \rangle} [1 + v \delta(\sigma_i, \sigma_j)], \quad (\text{E8})$$

where $v = e^\beta - 1$. We now expand the product in the spirit of the Fortuin-Kasteleyn expansion [27,28], yielding 2^E terms,

where E is the number of edges of the net lattice:

$$\dots = \frac{1}{Z} \left(\underbrace{\sum_{\{\sigma\}} O_{\vec{x}}(\{\sigma\})}_{\text{Diagram 1}} + v \underbrace{\sum_{\{\sigma\}} O_{\vec{x}}(\{\sigma\}) \delta(\sigma_1, \sigma_2) + \dots}_{\text{Diagram 2}} \right). \quad (\text{E9})$$

Here we have associated subgraphs G' of the net lattice G to each of the terms in the expansion, where G' has an edge between i and j if the expansion term contains $\delta(\sigma_i, \sigma_j)$. Let us investigate each sum individually. The first sum runs over Q^4 configurations. In Q^3 of those, $\sigma_{\vec{x}_a} = \sigma_{\vec{x}_b}$, implying $O_{\vec{x}}(\{\sigma\}) = 1$. In the other $Q^3(Q-1)$ terms, $\sigma_{\vec{x}_a} \neq \sigma_{\vec{x}_b}$ and $O_{\vec{x}}(\{\sigma\}) = (1+Q)/(1-Q)$. Therefore the sum evaluates to

$$\sum_{\{\sigma\}} O_{\vec{x}}(\{\sigma\}) = Q^3 + Q^3(Q-1) \frac{1+Q}{1-Q} = -Q^4. \quad (\text{E10})$$

The second sum contains Q^3 configurations and because there is a δ -function between spins 1 and 2, $\sigma_{\vec{x}_a} = \sigma_{\vec{x}_b}$ in all of them,

$$\sum_{\{\sigma\}} O_{\vec{x}}(\{\sigma\}) \delta(\sigma_1, \sigma_2) = Q^3. \quad (\text{E11})$$

Adding all these of contributions yields

$$\langle O_{\vec{x}} \rangle = \frac{1}{Z} \sum_{G' \subseteq G} Q^{n(G')} v^{b(G')} \tilde{O}_{\vec{x}}(G'), \quad (\text{E12})$$

where $n(G')$ is the number of connected components in G' , $b(G')$ is the number of bonds and

$$\tilde{O}_{\vec{x}}(G') = \begin{cases} 1 & \text{if } G' \text{ has a link at } \vec{x} \\ -1 & \text{otherwise.} \end{cases} \quad (\text{E13})$$

Each subgraph G' of the net lattice can be associated to a unique loop pattern $L(G')$ on the square lattice (Fig. 7), such that for the number of closed loops, we have

$$n_{L(G')} = n(G') + c(G') \quad \text{and} \quad (\text{E14})$$

$$\tilde{O}_{\vec{x}}(G') = \langle L(G') | \tilde{\sigma}_z(\vec{x}) | L(G') \rangle, \quad (\text{E15})$$

where $c(G')$ is the number of circuits in G' . Plugging Euler's relation

$$n(G') = c(G') - b(G') - V, \quad (\text{E16})$$

with V the number of vertices in G and (E14) into (E12) yields

$$\begin{aligned} \langle O_{\vec{x}} \rangle &= \frac{1}{Z} \sum_{G' \subseteq G} \sqrt{Q}^{n(G')} \sqrt{Q}^{b(G')} v^{b(G')} \tilde{O}_{\vec{x}}(G') \\ &= \frac{\sqrt{Q}^{-V}}{Z} \sum_{G' \subseteq G} \sqrt{Q}^{n(G')+c(G')} \left(\frac{v}{\sqrt{Q}} \right)^{b(G')} \tilde{O}_{\vec{x}}(G') \\ &= \frac{\sum_L \sqrt{Q}^{n_L} \left(\frac{v}{\sqrt{Q}} \right)^{b(G')} \langle L | \tilde{\sigma}_z(\vec{x}) | L \rangle}{\sum_L \sqrt{Q}^{n_L} \left(\frac{v}{\sqrt{Q}} \right)^{b(G')}} \end{aligned}$$

$$\begin{aligned} & \xrightarrow{\beta \rightarrow \ln(1+\sqrt{Q})} \frac{\sum_L \sqrt{Q}^{n_L} \langle L | \tilde{\sigma}_z(\vec{x}) | L \rangle}{\sum_L \sqrt{Q}^{n_L}} \\ & \xrightarrow{Q \rightarrow 16} \frac{\langle \psi | \tilde{\sigma}_z(\vec{x}) | \psi \rangle}{\langle \psi | \psi \rangle}. \end{aligned} \quad (\text{E17})$$

This argument can be repeated for the correlator

$$\langle O_{\vec{x}} O_{\vec{y}} \rangle = \frac{\langle \psi | \tilde{\sigma}_z(\vec{x}) \tilde{\sigma}_z(\vec{y}) | \psi \rangle}{\langle \psi | \psi \rangle}, \quad (\text{E18})$$

thereby showing that

$$C[\vec{x}, \vec{y}] = \langle O_{\vec{x}} O_{\vec{y}} \rangle - \langle O_{\vec{x}} \rangle \langle O_{\vec{y}} \rangle, \quad (\text{E19})$$

i.e., the staggered σ_z correlation function in the $\lambda = 1$ -PEPS is equal to the link-link correlation of a classical $Q = 16$ Potts model at $\beta = \ln(1 + \sqrt{Q})$. The model is known to undergo a phase transition at that point for all values of Q . While this transition is critical for $Q \leq 4$ [21–23, 29–34], it is of first order for $Q > 4$ [35, 36], implying that the local correlator (E19) decays exponentially, proving (E4). ■

A more general, alternative proof invokes the mapping between the norm of the PEPS to a Potts partition function. To this end, define the tensor network using tensors (8) with independent variables on every site, i.e.,

$$|\psi(\lambda_{(1,1)}, \lambda_{(1,2)}, \dots, \lambda_{(N_h, N_v)})\rangle =: |\psi(\vec{\lambda})\rangle, \quad (\text{E20})$$

Taking derivatives with respect to different λ will yield the expectation value of some local diagonal operator acting on, e.g., one site, $D_{\text{PEPS}}(\vec{x})$,

$$\frac{\partial}{\partial \lambda_{\vec{x}}} \ln \langle \psi(\vec{\lambda}) | \psi(\vec{\lambda}) \rangle = \frac{\langle \psi(\vec{\lambda}) | D_{\text{PEPS}}(\vec{x}) | \psi(\vec{\lambda}) \rangle}{\langle \psi | \psi \rangle}. \quad (\text{E21})$$

Introducing the effective coupling strengths $\vec{\beta}$ via

$$\lambda_{\vec{x}} = \begin{cases} \sqrt{\frac{e^{\beta_{\vec{x}}} - 1}{\sqrt{Q}}} & \text{if } \vec{x} \text{ is on the even sublattice} \\ \sqrt{\frac{\sqrt{Q}}{e^{\beta_{\vec{x}}} - 1}} & \text{if } \vec{x} \text{ is on the odd sublattice,} \end{cases} \quad (\text{E22})$$

one can directly calculate that

$$\langle \psi(\vec{\lambda}) | \psi(\vec{\lambda}) \rangle = C(\vec{\beta}) \underbrace{\sum_L \sqrt{Q}^{n_L} \prod_{\vec{x}} \left(\frac{e^{\beta_{\vec{x}}} - 1}{\sqrt{Q}} \right)^{b_{\vec{x}}(L)}}_{Z_{\text{inhom Potts}}}, \quad (\text{E23})$$

where $b_{\vec{x}}(L)$ is 1 if $G'(L)$ has a bond at \vec{x} and 0 otherwise. Here, $Z_{\text{inhom Potts}}$ is the partition function of a Potts model with different effective couplings between every pair of spins, given by (E22). The constant is given by

$$C(\vec{\beta}) = \prod_{\vec{x} \text{ odd}} \left(\frac{e^{\beta_{\vec{x}}} - 1}{\sqrt{Q}} \right). \quad (\text{E24})$$

Therefore

$$\frac{\langle \psi(\vec{\lambda}) | D_{\text{PEPS}}(\vec{x}) | \psi(\vec{\lambda}) \rangle}{\langle \psi | \psi \rangle} = \frac{\partial \beta_{\vec{x}}}{\partial \lambda_{\vec{x}}} \frac{\partial}{\partial \beta_{\vec{x}}} \ln(C(\vec{\beta}) Z_{\text{inhom Potts}}). \quad (\text{E25})$$

As usual, taking logarithmic derivatives of the partition function will yield some classical observable $D_{\text{Potts}}(\vec{x})$:

$$\dots = \langle D_{\text{Potts}}(\vec{x}) \rangle. \quad (\text{E26})$$

In particular, the point $\vec{\lambda} = \vec{1}$ corresponds to the original Potts model at its phase transition with all coupling strengths equal,

$$\langle D_{\text{PEPS}}(\vec{x}) \rangle_{\lambda=1} = \langle D_{\text{Potts}}(\vec{x}) \rangle_{\beta=1+\sqrt{Q}}. \quad (\text{E27})$$

Taking higher derivatives yields three-point and higher-order correlators. In our case, $Q = 16$ and all such operators decays exponentially even at the phase transition. This argument can be expanded by linearity to conclude that all diagonal correlators of the PEPS must decay exponentially.

Finally, for $u \neq 0$, the mapping has to be carried out with respect to two *coupled* Potts models, whose phase diagram is also known [37–39]. As the nature of the phase transition remains unchanged, we expect the correlation function to behave in the same manner as derived above.

APPENDIX F: OPEN BOUNDARY CONDITIONS AND UNIQUE GROUND STATE

In Sec. III B, we prove that the ground state of a modified parent Hamiltonian is unique. The key step in the proof is the fact that the minimal connectivity pattern can be reached from arbitrary starting loop patterns.

Claim. For every loop pattern L , there exists a sequence Σ of bulk moves (33) and boundary moves (43), such that

$$p(\Sigma(L)) = p_{\min}, \quad (\text{F1})$$

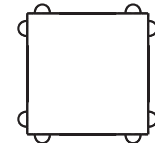
where p_{\min} is given by (44).

Proof. We are going to construct Σ explicitly, starting from an arbitrary loop pattern L . We begin in the top left corner. Combining boundary moves on the first horizontal and vertical dominos and potentially a bulk move on the plaquette in the top left corner, we can transform the top left corner of L into



$$. \quad (\text{F2})$$

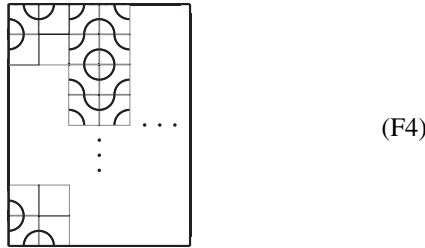
We proceed similarly for all other corners:



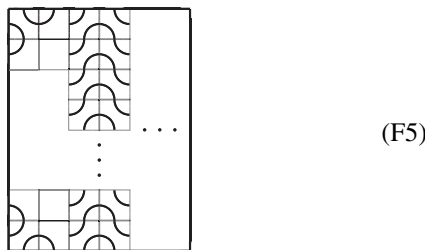
$$. \quad (\text{F3})$$

Now we continue sequentially, column by column. If the top domino looks like $\begin{array}{|c|c|} \hline \square & \square \\ \hline \end{array}$ or $\begin{array}{|c|c|} \hline \square & \square \\ \hline \end{array}$, transform it into $\begin{array}{|c|c|} \hline \square & \square \\ \hline \end{array}$ using (43). If it is in the $\begin{array}{|c|c|} \hline \square & \square \\ \hline \end{array}$ state, we will see now that the corresponding plaquette can be brought into the $|B\rangle$ state, after which the bubble is cut off and the boundary move is applicable again.

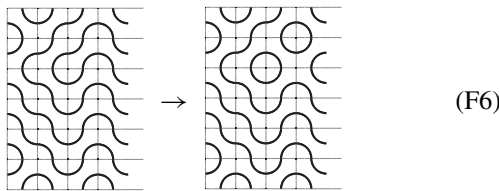
There are two scenarios. In the first, the top $\begin{smallmatrix} \square & \square \\ \square & \square \end{smallmatrix}$ -domino has a bubble or tadpole underneath it:



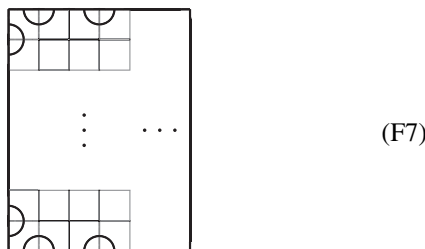
In this case, the bubble can be moved up to the topmost plaquette using bulk moves. It can then be cut off to transform the top domino into $\begin{smallmatrix} \square & \square \\ \square & \square \end{smallmatrix}$. In the second scenario, there is no bubble or tadpole in the column:



Then, there must necessarily be N_v paths passing through the column left to right. Only $N_v - 4$ of them can originate from the west boundary, since $4 + 4k$ out of the $N_v + 4k$ boundary points to the left of the k th column are already connected with their nearest neighbours. Therefore, at least two pairs of paths must actually be a single path, which has a tadpole to the left of the column. This tadpole can be moved into the column upon which we recover situation 1, e.g.,



The bottom tile is transformed into $\begin{smallmatrix} \square & \square \\ \square & \square \end{smallmatrix}$ in the same manner to arrive at

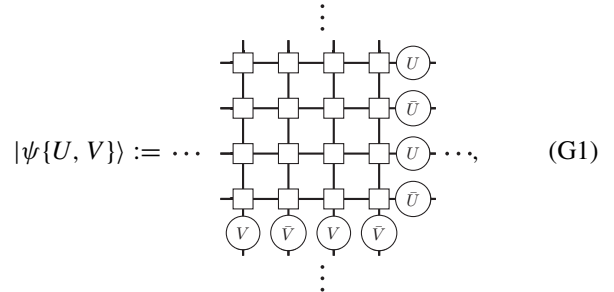


After fixing the top and bottom dominos column by column, we apply the same procedure to the left and right boundary. Evidently, once a boundary domino is in the correct state (e.g., $\begin{smallmatrix} \square & \square \\ \square & \square \end{smallmatrix}$ for top dominos), it will never be touched again

during this procedure, allowing us to sequentially bring the connectivity pattern into minimal form. ■

APPENDIX G: DIMENSION OF THE STRING-INSERTED SUBSPACE

Let N_h, N_v be even and define



where the boxes are A tensors defined in Eq. (8) and periodic boundary conditions are enforced such that the tensor network lives on an $N_h \times N_v$ torus (we have dropped the subscript indicating the system size for better readability in the following). Note that one has to complex conjugate every other unitary in order for one to be able to pull the strings through a row or column of tensors, respectively. If U and V commute, these strings can be moved freely through the system and it follows that $H|\psi\{U, V\}\rangle = 0$ for the parent Hamiltonian defined in (29). The purpose of this section is to compute the dimension of this *string-inserted* subspace of the ground state manifold:

$$S' := \text{span}\{|\psi\{U, V\}\rangle \mid [U, V] = 0, U, V \in SU(2)\}. \quad (G2)$$

We will show that

$$\dim S' = \frac{(N_h + 1)(N_v + 1) + 1}{2}. \quad (G3)$$

To this end, it is useful to make the following definition.

Definition. For a tuple of $(j, k) \in \mathbb{Z}^2$, define

$$g(j, k) = \begin{cases} \gcd(j, |k|) & \text{if } j, k \neq 0 \\ j & \text{if } k = 0, j > 0 \\ |k| & \text{if } j = 0, |k| > 0 \\ 1 & \text{if } k = j = 0 \end{cases}. \quad (G4)$$

We make the following observations. (1) The winding number of a nontrivial loop in, say, the horizontal direction is equivalent to the difference of how many times that loop crosses the U subset of the right boundary versus how many times it crosses the \bar{U} subset of the right boundary. These are the odd and even points on the boundary, respectively, as shown in (G1). An equivalent statement holds for nontrivial winding in the vertical direction. (2) If in a given loop pattern L there is a loop winding nontrivially around the torus j times in the horizontal direction and k times in the vertical direction, then *all* nontrivial loops have winding number (j, k) or $(-j, -k)$ (in fact, half of the loops will have winding number (j, k) and the other half $(-j, -k)$). Therefore we may denote the winding sector of such a loop pattern by $W(L) = (j, k)$. To remove ambiguity, we enforce $j \geq 0$. (3) A loop cannot wind around the torus (j, k) times if $g(j, k) \neq 1$. (4) A loop pattern in a given winding sector (j, k) , can have $n_{NTL} \in \{2, 4, \dots, \min\{\lfloor N_h/j \rfloor, \lfloor N_v/k \rfloor\}\}$ nontrivial loops. Therefore we redefine the winding sector of a loop pattern that has

$n_{NTL}/2$ loops wrapping around the torus (j, k) times and $n_{NTL}/2$ loops wrapping around the torus $(-j, -k)$ times as $W(L) = (j \times n_{NTL}/2, k \times n_{NTL}/2)$.

We are now ready for some helpful definitions and shorthand notations.

Definition.

$$\widetilde{N}_h := N_h + 1, \quad (\text{G5})$$

$$\widetilde{N}_v := N_v + 1. \quad (\text{G6})$$

Definition.

$$|j, k\rangle := \sum_{\substack{L \text{ s.t.} \\ W(L)=(j,k)}} 2^{nL} |L\rangle. \quad (\text{G7})$$

By the orthogonality of the physical basis states, different $|j, k\rangle$ are clearly orthogonal:

$$\langle j, k | j', k' \rangle := \delta_{jj', kk'} |||j, k\rangle|^2 \quad (\text{G8})$$

and by the above observations $|||j, k\rangle|^2 \neq 0$ for all $(j, k) \in I$.

Definition.

$$D_\phi = \begin{pmatrix} e^{i\phi} & 0 \\ 0 & e^{-i\phi} \end{pmatrix}, \quad (\text{G9})$$

$$W_{N_v}(\phi) := \bigotimes_{i=1}^{N_v/2} D_\phi \otimes \bar{D}_\phi, \quad (\text{G10})$$

$$\tilde{W}_{N_v}^l := W_{N_v} \left(\frac{\pi l}{\widetilde{N}_v} \right). \quad (\text{G11})$$

Definition.

$$|\psi_{\phi, \theta}\rangle := |\psi\{D_\phi, D_\theta\}\rangle, \quad (\text{G12})$$

$$|\tilde{\psi}_{l, m}\rangle := |\psi_{\phi = \frac{\pi l}{\widetilde{N}_v}, \theta = \frac{\pi m}{\widetilde{N}_h}}\rangle. \quad (\text{G13})$$

Definition.

$$I = \left\{ (x, y) \mid x = 0, \dots, N_v/2, \right. \\ \left. \begin{array}{ll} y = 0, \dots, N_h/2 & \text{if } x = 0 \\ y = -N_h/2, \dots, N_h/2 & \text{if } x \neq 0 \end{array} \right\}. \quad (\text{G14})$$

Counting the number of elements in I reveals that

$$|I| = \frac{(N_h + 1)(N_v + 1) + 1}{2}. \quad (\text{G15})$$

Definition.

$$|\phi_{k_x, k_y}\rangle := \frac{1}{\widetilde{N}_v \widetilde{N}_h} \sum_{l=0}^{N_v} \sum_{m=0}^{N_h} e^{2\pi i \left(\frac{k_x l}{\widetilde{N}_v} + \frac{k_y m}{\widetilde{N}_h} \right)} |\tilde{\psi}_{l, m}\rangle. \quad (\text{G16})$$

Definition.

$$M_{(jk), (lm)} := \left[2 \cos \left(\frac{\pi j l}{g(j, k) \widetilde{N}_v} + \frac{\pi k m}{g(j, k) \widetilde{N}_h} \right) \right]^{2g(j, k)} \quad (\text{G17})$$

for any set of integers j, k, l , and m .

Claim.

$$\dim \mathcal{S}' \leq |I|. \quad (\text{G18})$$

Claim.

$$\dim \mathcal{S}' \geq |I|. \quad (\text{G19})$$

Together, (G18), (G19), and (G15) entail that

$$\dim \mathcal{S}' = \frac{(N_h + 1)(N_v + 1) + 1}{2}. \quad (\text{G20})$$

Proof. To prove (G18) starting from the definition of \mathcal{S}' , we can first restrict the unitaries U and V to be diagonal, i.e.,

$$\mathcal{S}' = \text{span}\{|\psi_{\phi, \theta}\rangle \mid \phi, \theta \in [0, 2\pi]\}. \quad (\text{G21})$$

This is because any state that is generated by nondiagonal U and V is related to a state with U and V diagonal by conjugating the whole network with S , where S is the unitary that simultaneously diagonalises U and V . Because of the fundamental symmetry of the PEPS tensor, this conjugation leaves the state invariant.

As a first step, we are going to show that

$$\mathcal{S}' = \text{span}\{|\tilde{\psi}_{l, m}\rangle\}_{\substack{l=0, \dots, N_v \\ m=0, \dots, N_h}}. \quad (\text{G22})$$

Because $|\psi_{\phi, \theta}\rangle$ depends linearly on $W_{N_v}(\phi) \otimes W_{N_h}(\theta)$, it is sufficient to show that

$$\text{span}\{W_{N_v}(\phi) \otimes W_{N_h}(\theta)\} \\ = \text{span}\{\tilde{W}_{N_v}^l \otimes \tilde{W}_{N_h}^m\}_{\substack{l=0, \dots, N_v \\ m=0, \dots, N_h}}. \quad (\text{G23})$$

Clearly,

$$\text{span}\{W_{N_v}(\phi) \otimes W_{N_h}(\theta)\} \\ \supseteq \text{span}\{\tilde{W}_{N_v}^l \otimes \tilde{W}_{N_h}^m\}_{\substack{l=0, \dots, N_v \\ m=0, \dots, N_h}}, \quad (\text{G24})$$

and we will prove the reverse inclusion by showing that

$$\widetilde{N}_v \widetilde{N}_h \geq \dim \text{span}\{W_{N_v}(\phi) \otimes W_{N_h}(\theta)\} \\ \geq \dim \text{span}\{\tilde{W}_{N_v}^l \otimes \tilde{W}_{N_h}^m\}_{\substack{l=0, \dots, N_v \\ m=0, \dots, N_h}} \\ \geq \widetilde{N}_v \widetilde{N}_h. \quad (\text{G25})$$

The first inequality of (G25) follows by expanding the operator

$$W_{N_v}(\phi) = e^{iN_v\phi} \mathbf{1}_{\binom{N_v}{0}} \oplus e^{i(N_v-2)\phi} \mathbf{1}_{\binom{N_v}{1}} \oplus \dots \oplus e^{-iN_v\phi} \mathbf{1}_{\binom{N_v}{N_v}}, \quad (\text{G26})$$

which, for general values of ϕ spans an \widetilde{N}_v -dimensional space. The second inequality in (G25) is a trivial conclusion of (G24).

To see the validity of the third inequality, consider the matrix whose columns are made up of the distinct diagonal entries of

$\tilde{W}_{N_v}^l$ for $l = \frac{N_v}{2}, \frac{N_v}{2} - 1, \dots, 0, N_v, N_v - 1, \dots, \frac{N_v}{2} + 1$:

$$F_{N_v} = \begin{pmatrix} | & | & | & | \\ \text{diag}(\tilde{W}_{N_v}^{N_v/2}) & \text{diag}(\tilde{W}_{N_v}^{N_v/2-1}) & \dots & \\ | & | & | & | \\ 1 & 1 & 1 & 1 \\ 1 & \omega & \omega^2 & \omega^3 \\ 1 & \omega^2 & \omega^4 & \omega^6 & \dots \\ 1 & \omega^3 & \omega^6 & \omega^9 & \\ & \vdots & & \ddots & \end{pmatrix}, \quad (\text{G27})$$

which is simply \tilde{N}_v times the $\tilde{N}_v \times \tilde{N}_v$ discrete Fourier matrix [we have set $\omega = \exp(2\pi i/\tilde{N}_v)$], and therefore has full rank equal to \tilde{N}_v . Applying these arguments to both tensor factors individually yields (G25).

Finally, we will prove that

$$\text{span}\{|\tilde{\psi}_{l,m}\rangle\}_{\substack{l=0,\dots,N_v \\ m=0,\dots,N_h}} = \text{span}\{|\tilde{\psi}_{l,m}\rangle\}_{(l,m)\in I} \quad (\text{G28})$$

by showing that for each $(l, m) \notin I$, there exists an $(l', m') \in I$ such that $|\tilde{\psi}_{l,m}\rangle = |\tilde{\psi}_{l',m'}\rangle$. The key observation is that

$$|\psi\{U, V\}\rangle = |\psi\{XUX^\dagger, XVX^\dagger\}\rangle, \quad (\text{G29})$$

$$|\psi\{U, V\}\rangle = |\psi\{-U, V\}\rangle, \quad (\text{G30})$$

$$|\psi\{U, V\}\rangle = |\psi\{U, -V\}\rangle, \quad (\text{G31})$$

which follows from the fact that conjugating the whole tensor network with $iX \in SU(2)$ leaves the state invariant and the numbers of U s and V s are both even. Inserting $U = \text{diag}(\exp(\pi i l/\tilde{N}_v), \exp(-\pi i l/\tilde{N}_v))$ and $V = \text{diag}(\exp(\pi i m/\tilde{N}_h), \exp(-\pi i m/\tilde{N}_h))$, we obtain

$$|\tilde{\psi}_{l,m}\rangle = |\tilde{\psi}_{-l,-m}\rangle, \quad (\text{G32})$$

$$|\tilde{\psi}_{l,m}\rangle = |\tilde{\psi}_{l\pm\tilde{N}_v,m}\rangle, \quad (\text{G33})$$

$$|\tilde{\psi}_{l,m}\rangle = |\tilde{\psi}_{l,m\pm\tilde{N}_h}\rangle. \quad (\text{G34})$$

Using (G32)–(G34), for each $(l, m) \in [0, \dots, N_v] \times [0, \dots, N_h]$ we can now find an $(l', m') \in I$ such that $|\tilde{\psi}_{l,m}\rangle = |\tilde{\psi}_{l',m'}\rangle$, which imply (G28) and, together with (G22) show that

$$\dim \mathcal{S}' \leq |I|. \quad (\text{G35})$$

Proof. [Proof of (G19)] Because of (G22) and the $|\phi_{k_x, k_y}\rangle$ being linear combinations of the $|\tilde{\psi}_{l,m}\rangle$ via definition G, it is clear that

$$\mathcal{S}' \supseteq \text{span}\{|\phi_{k_x, k_y}\rangle\}_{(k_x, k_y) \in I}. \quad (\text{G36})$$

Also, from the observations made in the beginning of this section and (G7) and (G17), we see that

$$|\tilde{\psi}_{l,m}\rangle = \sum_{(j,k) \in I} M_{(jk), (lm)} |j, k\rangle. \quad (\text{G37})$$

The matrix elements of M can be simplified using the binomial theorem. For better readability, we are going to suppress the

argument of $g = g(j, k)$,

$$\begin{aligned} M_{(jk), (lm)} &= \left[2 \cos \left(\frac{j l \pi}{\tilde{N}_v g} + \frac{k m \pi}{\tilde{N}_h g} \right) \right]^{2g} \\ &= \left[e^{\frac{\pi i}{g} \left(\frac{j l}{\tilde{N}_v} + \frac{k m}{\tilde{N}_h} \right)} + e^{-\frac{\pi i}{g} \left(\frac{j l}{\tilde{N}_v} + \frac{k m}{\tilde{N}_h} \right)} \right]^{2g} \\ &= \sum_{a=0}^{2g} e^{\frac{2\pi i}{g} \left(\frac{j l}{\tilde{N}_v} + \frac{k m}{\tilde{N}_h} \right) (a-g)} \binom{2g}{a}. \end{aligned} \quad (\text{G38})$$

Plugging (G37) and (G38) into definition (G16) yields

$$\begin{aligned} |\phi_{(k_x, k_y)}\rangle &= \sum_{(j,k) \in I} \sum_{a=0}^{2g} \binom{2g}{a} |j, k\rangle \\ &\times \underbrace{\frac{1}{\tilde{N}_v} \sum_{l=0}^{N_v} \left[e^{\frac{2\pi i}{g} \left(\frac{j}{\tilde{N}_v} (a-g) - k_x \right) l} \right]}_{\delta_{\frac{j}{g} (a-g) - k_x \in \tilde{N}_v \mathbb{Z}}} \\ &\times \underbrace{\frac{1}{\tilde{N}_h} \sum_{m=0}^{N_h} \left[e^{\frac{2\pi i}{g} \left(\frac{k}{\tilde{N}_h} (a-g) - k_y \right) m} \right]}_{\delta_{\frac{k}{g} (a-g) - k_y \in \tilde{N}_h \mathbb{Z}}}. \end{aligned} \quad (\text{G39})$$

In principle, the constraints only enforce, e.g.,

$$\frac{k}{g} (a-g) - k_y = n \tilde{N}_h \quad (\text{G40})$$

for $n \in \mathbb{Z}$. However, we will now show that if $|n| \geq 1$, then it follows that $|a-g| > g$ which entails that either $a < 0$ or $a > 2g$, in both cases the summation on a will be empty. Rearranging (G40) and taking the absolute value yields

$$\begin{aligned} |a-g| &= \frac{|n \tilde{N}_h + k_y|}{|k|} g \\ &\geq \frac{|n| \tilde{N}_h - |k_y|}{|k|} g \\ &> \tilde{N}_h \frac{|n| - 1/2}{|k|} g \\ &> \frac{\tilde{N}_h}{2} \frac{2}{\tilde{N}_h} g \\ &= g, \end{aligned} \quad (\text{G41})$$

where we have used that $|a+b| > |a-b|$, $|n| \geq 1$, $|k_y| < N_h/2$ and $|k| < N_h/2$. This argument can be carried out for the constraints originating from both the summation over l and m , leaving us with

$$\frac{j}{g} (a-g) = k_x, \quad (\text{G42})$$

$$\frac{k}{g} (a-g) = k_y. \quad (\text{G43})$$

These equations mean that

$$|j, k| \phi_{(k_x, k_y)} = \begin{cases} \binom{2g}{k_x g / j + g} & \text{if } k_x / k_y = j / k \\ 0 & \text{otherwise} \end{cases}. \quad (\text{G44})$$

In particular, by orthogonality of the $|j, k\rangle$, sectors with different k_x/k_y are mutually orthogonal. As a final step, we will investigate the sector that is spanned by the vectors

$$\left\{ |\phi_{(k_x, k_y)}\rangle \right\}_{\substack{(k_x, k_y) \in I \\ k_x/k_y = p/q}} \quad (\text{G45})$$

for a fixed, completely reduced fraction p/q . The vectors in this set have the form $|\phi_{(p, q)}\rangle, |\phi_{(2p, 2q)}\rangle, \dots$. Since

$$\langle p, q | \phi_{(bp, bq)} \rangle = \binom{2}{b+1}, \quad (\text{G46})$$

only $|\phi_{(1p, 1q)}\rangle$ has nonzero overlap with $|p, q\rangle$. Therefore $|\phi_{(1p, 1q)}\rangle$ must necessarily be linearly independent from all other vectors in that sector. We can therefore remove $|\phi_{(1p, 1q)}\rangle$ from $\{|\phi_{(k_x, k_y)}\rangle\}_{(k_x, k_y) \in I, k_x/k_y = p/q}$ and check the remaining basis vectors for linear independence. Indeed, we can iterate this procedure to show that in the remaining set, there exists exactly one vector that has nonzero overlap with $|bp, bq\rangle$, which is $|\phi_{(bp, bq)}\rangle$. Therefore

$$\dim \text{span} \left\{ |\phi_{(k_x, k_y)}\rangle \right\}_{(k_x, k_y) \in I} = |I|, \quad (\text{G47})$$

and by Eq. (G36), it follows that

$$\dim S' \geq |I|. \quad (\text{G48})$$

■

-
- [1] D. Perez-Garcia, F. Verstraete, M. M. Wolf, and J. I. Cirac, *Quantum Inf. Comput.* **7**, 401 (2007).
- [2] N. Schuch, D. Pérez-García, and J. I. Cirac, *Phys. Rev. B* **84**, 165139 (2011).
- [3] D. J. Williamson, N. Bultinck, M. Mariën, M. B. Sahinoglu, J. Haegeman, and F. Verstraete, *Phys. Rev. B* **94**, 205150 (2016).
- [4] S. Bachmann and B. Nachtergaele, *Phys. Rev. B* **86**, 035149 (2012).
- [5] N. Schuch, J. I. Cirac, and D. Perez-Garcia, *Ann. Phys.* **325**, 2153 (2010).
- [6] O. Buerschaper, M. Aguado, and G. Vidal, *Phys. Rev. B* **79**, 085119 (2009).
- [7] M. B. Şahinoğlu, D. Williamson, N. Bultinck, M. Mariën, J. Haegeman, N. Schuch, and F. Verstraete, [arXiv:1409.2150](https://arxiv.org/abs/1409.2150) [quant-ph].
- [8] T. B. Wahl, H.-H. Tu, N. Schuch, and J. I. Cirac, *Phys. Rev. Lett.* **111**, 236805 (2013).
- [9] S. Yang, T. B. Wahl, H.-H. Tu, N. Schuch, and J. I. Cirac, *Phys. Rev. Lett.* **114**, 106803 (2015).
- [10] D. Poilblanc, *Phys. Rev. B* **96**, 121118 (2017).
- [11] N. D. Mermin and H. Wagner, *Phys. Rev. Lett.* **17**, 1133 (1966).
- [12] M. Fannes, B. Nachtergaele, and R. F. Werner, *Commun. Math. Phys.* **144**, 443 (1992).
- [13] G. Rumer, E. Teller, and H. Weyl, *Nachr. Ges. Wiss. Goettingen, Math.-Phys. Kl.* **1932**, 499 (1932).
- [14] R. Saito, *J. Phys. Soc. Jpn.* **59**, 482 (1990).
- [15] R. Pauncz, *Spin Eigenfunctions - Construction and Use* (Springer US, Plenum Press, New York, 1979).
- [16] E. Fradkin and J. E. Moore, *Phys. Rev. Lett.* **97**, 050404 (2006).
- [17] D. S. Rokhsar and S. A. Kivelson, *Phys. Rev. Lett.* **61**, 2376 (1988).
- [18] R. Moessner, S. L. Sondhi, and E. Fradkin, *Phys. Rev. B* **65**, 024504 (2001).
- [19] E. Ardonne, P. Fendley, and E. Fradkin, *Ann. Phys.* **310**, 493 (2004).
- [20] R. Moessner and S. L. Sondhi, *Phys. Rev. Lett.* **86**, 1881 (2001).
- [21] M. Troyer, S. Trebst, K. Shtengel, and C. Nayak, *Phys. Rev. Lett.* **101**, 230401 (2008).
- [22] P. Fendley, *Ann. Phys.* **323**, 3113 (2008).
- [23] P. Fendley, [arXiv:0711.0014](https://arxiv.org/abs/0711.0014) [cond-mat.stat-mech].
- [24] A. Nahum, J. T. Chalker, P. Serna, M. Ortuno, and A. M. Somoza, *Phys. Rev. B* **88**, 134411 (2013).
- [25] M. Fulmek, *Electron. J. Combinatorics* **14**, R64 (2007).
- [26] Philippe Flajolet and Robert Sedgewick, *Analytic Combinatorics* (Cambridge University Press, Cambridge, UK, 2009).
- [27] F. Y. Wu, *Rev. Mod. Phys.* **54**, 235 (1982).
- [28] C. M. Fortuin and P. W. Kasteleyn, *Physica* **57**, 536 (1972).
- [29] B. Nienhuis, in *Phase Transitions and Critical Phenomena*, edited by C. Domb and J. Lebowitz, Vol. 11 (Academic Press Ltd., London, UK, 1987).
- [30] P. Fendley, S. V. Isakov, and M. Troyer, *Phys. Rev. Lett.* **110**, 260408 (2013).
- [31] M. Freedman, *Commun. Math. Phys.* **234**, 129 (2003).
- [32] M. Freedman, C. Nayak, and K. Shtengel, *Phys. Rev. Lett.* **94**, 066401 (2005).
- [33] M. Freedman, C. Nayak, and K. Shtengel, *Phys. Rev. Lett.* **94**, 147205 (2005).
- [34] P. Fendley and E. Fradkin, *Phys. Rev. B* **72**, 024412 (2005).
- [35] V. Beffara and H. Duminil-Copin, *Probab. Theory Relat. Fields* **153**, 511 (2012).
- [36] H. Duminil-Copin, M. Gagnebin, M. Harel, I. Manolescu, and V. Tassion, [arXiv:1611.09877](https://arxiv.org/abs/1611.09877).
- [37] P. Fendley and J. L. Jacobsen, *J. Phys. A* **41**, 215001 (2008).
- [38] V. Dotsenko, J. L. Jacobsen, M.-A. Lewis, and M. Picco, *Nucl. Phys. B* **546**, 505 (1999).
- [39] V. Dotsenko, J. L. Jacobsen, X. S. Nguyen, and R. Santachiara, *Nucl. Phys. B* **631**, 426 (2002).